
Differentially Private Supervised Manifold Learning with Applications like Private Image Retrieval

Praneeth Vepakomma, Julia Balla, Ramesh Raskar

vepakom@mit.edu
Massachusetts Institute of Technology

Abstract

Differential Privacy offers strong guarantees such as immutable privacy under post processing. Thus it is often looked to as a solution to learning on scattered and isolated data. This work focuses on supervised manifold learning, a paradigm that can generate fine-tuned manifolds for a target use case. Our contributions are two fold. 1) We present a novel differentially private method *PrivateMail* for supervised manifold learning, the first of its kind to our knowledge. 2) We provide a novel private geometric embedding scheme for our experimental use case. We experiment on private "content based image retrieval" - embedding and querying the nearest neighbors of images in a private manner - and show extensive privacy-utility tradeoff results, as well as the computational efficiency and practicality of our methods.

1 INTRODUCTION

Privacy preserving computation enables distributed hosts with "siloes" away data to query, analyse or model their sensitive data and share findings in a privacy preserving manner. In this paper we focus on the problem of privately retrieving nearest neighbors of a client's query image with respect to a server's database of images. Consider the setting where a client would like to obtain the k-nearest matches to its query image from an external distributed database. Central to our approach is the use of state of the art image retrieval machine learning models such as [Matsui et al., 2020, Chen et al., 2021, Zhou et al., 2017, Dubey, 2020] for feature extraction. The nearest neighbors are retrieved using feature embeddings from distinct models trained/fine-tuned on premises of the client and the server respectively - each using their own datasets. The privacy that we aim to protect is with respect to the client's training data by protecting the

features obtained upon inference from the server's image retrieval model. We do this by geometrically embedding these features via a supervised manifold learning query that we propose. We then propose a differentially private mechanism to release the outputs of this query. The privatized outputs of this query are used to perform the matching and retrieval of the nearest neighbors in this privatized feature space.

Differential privacy [Dwork et al., 2014] is the formal notion of mathematical privacy that we guarantee through our mechanism of privately releasing supervised manifold learning queries. Differential privacy aims to prevent membership inference attacks [Shokri et al., 2017, Truex et al., 2018, Li and Zhang, 2020, Song et al., 2019, Shi et al., 2020] but an equivalence which shows that differential privacy mechanisms can also prevent reconstruction attacks under constraints on the level of utility that can be achieved have been shown in [Dwork et al., 2017, Garfinkel et al., 2018]. In this paper, we propose a differentially private method such that the training data used to train these deep learning models used for matching and retrieval are protected from membership inference attacks. Currently cryptographic methods for the problem of information retrieval were studied in works like [Xia et al., 2015]. These methods ensure to protect clients query via homomorphic encryption and oblivious transfer. These methods although comes with an impractical tradeoff of computational scalability especially when the size of the server's database is large, as is always the case in practice and when the feature size is high-dimensional [Elmehdwi et al., 2014, Lei et al., 2019, Yao et al., 2013].

1.0.1 Motivation

1. Cryptographic methods with strong security guarantees are currently not scalable computationally, for secure k-nn queries [Elmehdwi et al., 2014, Lei et al., 2019, Yao et al., 2013] especially when the number of records in the server-side database is large as is typically the case in real-life scenarios.

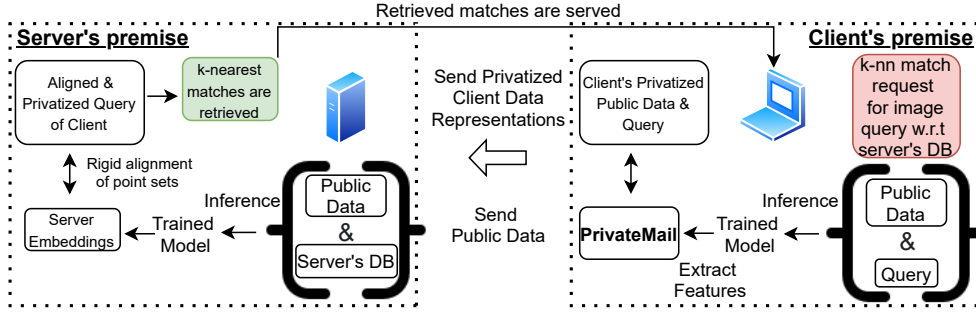


Figure 1: This illustration shows the lifecycle of interactions between client and server side entities for private image retrieval in the context of machine learning, starting from the red bubble on the right. At first, the client and server train a good on-premise machine learning model that is tailored for image retrieval. The client extracts features from this model on the query image and a public dataset. The extracted features go through the proposed Private-Mail for embedding them via locally differentially private (LDP) supervised manifold learning. These LDP embeddings are aligned at the server prior to performing the nearest-neighbor retrieval of matches that are served back to the client. The privatized representation of public dataset is used as an anchor in order to align the feature embeddings between the client and server.

2. Scalable systems for more specialized adjacent applications such as for biometric face or eye based authentication do exist [Boddeti, 2018, Engelsma et al., 2020], but they do not release any of the exact matches that were retrieved to the querying client. They just ascertain the existence of a match as an authenticating solution although this solution itself is an exact (non-randomized) solution. This thereby leaves room for membership inference attacks. We do not want to even remotely insinuate that cryptographic methods are weak. They are in fact, one of the strongest known notions of formal security to date. We just want to point out an artifact of the differences in what is protected by cryptographic methods versus differential privacy; both of which are popular yet formal approaches.
3. Cryptographic methods fundamentally guarantee protection of the computation that is performed in an encrypted domain. On the other hand, when the final result of k-nearest neighbor matches are served back to the client as exact solutions, it leaves room for membership inference attacks. These attacks are prevented by the approach of differential privacy, yet another popular and formal notion of mathematical privacy.
4. Currently available differential privacy solutions for biometric applications where content based matching of records is performed in [Steil et al., 2019, Chamikara et al., 2020] are either based on **a.)** a small number of hand-crafted features where the noise is calibrated on a per-record basis or on **b.)** based on older feature extraction regimes such as EigenFaces [Turk and Pentland, 1991]. EigenFaces are based on the classical linear dimensionality reduction method of principal components analysis, which is also an unsupervised method. We instead consider state of the art feature extraction used by recent deep learning architectures specialized

for image retrieval such as [Jun et al., 2019]. Our proposed query for supervised manifold learning that we formally privatize via our proposed approach of PrivateMail, instead preserves the nonlinear geodesics unlike PCA and instead operates in the supervised regime. The noise in our case is calibrated by treating the query as a matrix-variate query; thereby allowing for correlated noise in the dimensions that matter.

2 CONTRIBUTIONS

1. The main contribution of our paper is a differentially private method called ‘PrivateMail’ for the private release of outputs from a specific supervised manifold learning query.
2. The supervised manifold learning query that we use to geometrically embed features extracted from deep networks, is novel in itself. That said, we would only consider this as a secondary contribution to this paper.
3. The application that we test our scheme on is for differentially private ‘content based image retrieval’ where the k-nearest neighbors of an image query requested by a client are retrieved from a server’s database while maintaining differential privacy. We apply ‘PrivateMail’ to release the representations learnt by the machine learning model in order to perform the nearest neighbor query in the privatized representation space. We show the privacy utility tradeoffs of our approach in detail in the section on performance evaluation.

3 RELATED WORK

Non-private image search and retrieval: Current state of the art pipelines for content based image retrieval under the

non-private setting are fairly matured and based on nearest neighbor queries performed over state of the art deep feature representations of these images.

The query image and the database of images are compared in this learnt representation space. A detailed set of tutorials and surveys on this problem in the non-private setting is provided in [Matsui et al., 2020, Chen et al., 2021, Zhou et al., 2017, Dubey, 2020].

Private manifold learning: There have been recent developments in learning private geometric embeddings with differentially private unsupervised manifold learning. A notable example is the popular approach by [Arora and Upadhyay, 2019] for differentially private Laplacian Eigenmaps. Furthermore, the work in [Choromanska et al., 2016] provides a method for differentially private random projection trees to perform unsupervised private manifold learning. However none of these works consider the setting of differentially private manifold learning in the supervised setting - which we explore in this paper.

Secure k-nearest neighbor methods: Methods for secure k-nn such as [Elmehdwi et al., 2014, Lei et al., 2019, Yao et al., 2013] are currently not scalable on this problem for practical purposes yet especially when the number of records in the server-side database is large as is typically the case in real-life scenarios.

Cryptographic private information retrieval: PIR schemes introduced by Chor et al. [1995] look at the problem of devising a communication protocol involving just two parties, the database and the user, each having a secret input of data records $r_1, r_2 \dots r_n$ and a query record q respectively such that the user can retrieve a record r_i from the database, while keeping i private from this database entity. These schemes protect the privacy of the querier’s record, while the server’s privacy is not protected in the sense that the retrieved results are exact from the perspective of membership inference attacks. Information theoretic PIR schemes require replication of data across multiple servers.

Informally private/empirical CBIR in computer vision: Some earlier empirical works on informally private versions of this problem were studied in the context of image data in [Shashank et al., 2008].

3.1 DIFFERENTIAL PRIVACY

3.1.1 Preliminaries

Definition 1 (ϵ -Local Randomizer [Dwork et al. [2014]]). *Let $A : D \mapsto Y$ be a randomized algorithm mapping a data entry in data domain D to Y . The algorithm A is an ϵ -local randomizer if for all data entries $d, d' \in D$ and all outputs $y \in Y$, we have $-\epsilon \leq \ln \left(\frac{\Pr[A(d)=y]}{\Pr[A(d')=y]} \right) \leq \epsilon$.*

Definition 2 (Local Differential Privacy [Dwork et al., 2014]). *Let $A : D_n \mapsto Z$ be a randomized algorithm map-*

ping a dataset with n records to some arbitrary range Z . The algorithm A is ϵ -local differentially private if it can be written as $A(d_1, \dots, d_n) = \phi(A_1(d_1), \dots, A_n(d_n))$ where each $A_i : D \mapsto Y$ is an ϵ -local randomizer for each $i \in [n]$ and $\phi : Y_n \mapsto Z$ is some post-processing function of the privatized records $A_1(d_1), \dots, A_n(d_n)$. Note that the post-processing function does not have access to the raw data records.

3.1.2 Post-Processing Invariance

Differential privacy is immune to post-processing, meaning that an adversary without any additional knowledge about the dataset D cannot compute a function on the output $\mathcal{A}(D)$ to violate the stated privacy guarantees. Formally, for a deterministic function $g : \mathbb{R} \mapsto \mathbb{R}'$ and any event $S' \subseteq \mathbb{R}'$ we have $\Pr[g(\mathcal{A}(D)) \in S'] \leq e^\epsilon \Pr[g(\mathcal{A}(D')) \in S'] + \delta$ for any two neighboring datasets D and D' .

4 SUPERVISED MANIFOLD LEARNING QUERIES

In this section we present a way to perform supervised manifold learning and derive an optimization update for it. Our approach in this section is motivated by a.) the supervised manifold learning framework in [Vural and Guillemot, 2017], b.) the popular unsupervised manifold learning methods of [Belkin and Niyogi, 2003, Coifman and Lafon, 2006, Donoho and Grimes, 2003, Van der Maaten and Hinton, 2008] and c.) by the fact that differentially private mechanisms exist only for the unsupervised versions [Arora and Upadhyay, 2019, Choromanska et al., 2016].

4.0.1 Manifold learning: A geometric viewpoint

Manifold learning is a discrete analogue of the continuous problem of learning a map $f : \mathcal{M} \mapsto \mathbb{R}^d$ from a smooth, compact high dimensional Riemannian manifold such that for any two points x_1, x_2 on \mathcal{M} the geodesic distance on the manifold, $d_{\mathcal{M}}(x_1, x_2)$ is approximated by the Euclidean distance $\|f(x_1) - f(x_2)\|$ in \mathbb{R}^d . Different manifold learning techniques vary in their tightness of this approximation on varying datasets. Manifold learning techniques like ISOMAP, Laplacian Eigenmaps, Diffusion Maps, Hessian Eigenmaps aim to find a tighter approximation by trying to minimize a relevant bounding quantity b such that $\|f(x_1) - f(x_2)\| \leq B \cdot d_{\mathcal{M}}(x_1, x_2) + o(d_{\mathcal{M}}(x_1, x_2))$. Different techniques propose different possibilities for such a b . For example, Laplacian Eigenmaps uses $B = \|\nabla f(x_1)\|$ for which it is shown that the relation still holds as

$$\|f(x_1) - f(x_2)\| \leq \|\nabla f(x_1)\| \cdot \|x_1 - x_2\| + o(\|x_1 - x_2\|)$$

Hence, controlling $\|\nabla f\|_{L^2(\mathcal{M})}$ preserves geodesic relations on the manifold in the Euclidean space after the embedding.

This quantity of $\|\nabla f\|_{L^2(M)}$ in the continuous domain can be optimized via choosing the eigenfunctions of the Laplace-Beltrami operator in order to get the optimal embedding. This is explained in a series of papers by [Jones et al., 2008, Giné et al., 2006]. From a computational standpoint we note that

$$\sum_{i,j} \|z_i - z_j\|^2 \cdot W_{ij} = \text{Tr}(\mathbf{Z}^T L_X \mathbf{Z})$$

is the discrete version of $\|\nabla f\|_{L^2(M)}$. Therefore the equivalent solution to map $\{x_1, \dots, x_n\} \subset \mathbb{R}^p$ while preserving locality into $\{z_1, \dots, z_n\} \subset \mathbb{R}^d$ is to minimize this objective function for a specific graph Laplacian L_X that we describe below. Note that to simplify notation we refer to $L(X, \sigma)$ with L_X throughout the paper. A popular graph Laplacian, under which the above results were studied is that of graphs whose adjacency matrices are represented by the Gaussian kernel given by

$$\mathbf{L}(\mathbf{X}, \sigma)_{ik} = \begin{cases} \sum_{k \neq i} e^{-\frac{\|x_i - x_k\|^2}{\sigma}} & \text{if } i = k \\ -e^{-\frac{\|x_i - x_k\|^2}{\sigma}} & \text{if } i \neq k \end{cases} \quad (1)$$

where the scalar σ in here is also referred to as kernel bandwidth. [Giné et al., 2006, Belkin and Niyogi, 2005, 2007] show that this discrete Graph Laplacian converges to the Laplace-Beltrami operator. Therefore minimizing this over $\{Z^T D Z = I\}$ to avoid a trivial solution of $\text{Tr}(Z^T L_X Z) = 0$ is equivalent to setting Z to be the eigenvectors of L_X . An alternative for a faster solution is to define a linear constraint proposed in [Vepakomma and Elgammal, 2016] given by $\text{Tr}(Z^T S Q) = v$ where the scalar parameter $v \neq 0$, $S = \text{Laplacian}(1_{n \times n})$ is a graph Laplacian formed over an adjacency matrix of all 1's and Q denotes a Gaussian random matrix. This makes it a linearly constrained quadratic optimization problem where the Hessian of the objective is positive semi-definite, thereby leading to fast solutions via this relaxation.

The matrix $\mathbf{S}_{n \times n}$ is given by:

$$\mathbf{S}_{ij} := \begin{cases} -1 & \text{if } i \neq j \\ (n-1) & \text{if } i = j \end{cases} \quad (2)$$

The matrix $\mathbf{Q}_{n \times d}$ is a matrix with very trivial requirement of all rows being distinct (i.e, differ by at least one entry) and for practical purposes we choose a \mathbf{Q} through sampling the entries \mathbf{Q}_{ij} from an i.i.d Normal distribution or Bernoulli distribution. It has been shown in [Vural and Guillemot, 2017] that this formulation can be extended to the case of supervised manifold learning by posing the objective function as a difference of these terms and use a spectral solution as below.

$$f(\mathbf{Z}) = \text{Tr}(\mathbf{Z}^T L_X \mathbf{Z}) - \alpha \text{Tr}(\mathbf{Z}^T L_Y \mathbf{Z}) \quad (3)$$

The spectral solution to optimize this under orthonormal constraints $\mathbf{Z}^T \mathbf{Z} = \mathbf{I}$ results in a solution being the largest eigenvectors of $L_X - \alpha L_Y$.

4.1 OPTIMIZATION

In our initial contribution, we show that the relaxation in [Vepakomma and Elgammal, 2016] can be used on the above supervised manifold learning objective as well for a computationally more efficient solution which we then formally privatize in the next section as part of the main contribution of this paper. With regards to the computational efficiency we show that the problem can be posed as a difference of convex functions (DC optimization problem) in the following subsection. The benefit of this regime is that the optimization updates do not require a step-size parameter unlike in popular gradient based methods. We then further enhance its computational efficiency by providing a solution that instead only requires inversion of a diagonal matrix as opposed to the square matrix inversion needed in the case of the DC optimization update. Note that DC optimization problems have also been referred to as those that can be optimized with Concave-Convex procedure (CCCP). In fact, these problems are a special case of problems called Majorization-Minimization (or MM) problems. In fact, the popular EM algorithm is also a special case of MM algorithm.

4.1.1 Concave-convex procedure: Special case of majorization minimization

A function $g(\mathbf{Z}_{t+1}, \mathbf{X}_t)$ is said to majorize the function $f(\mathbf{Z})$ at \mathbf{Z}_t provided $f(\mathbf{Z}_t) = g(\mathbf{Z}_t, \mathbf{Z}_t)$ and $f(\mathbf{X}_t) \leq g(\mathbf{X}_t, \mathbf{Z}_{t+1})$ always holds true. The MM iteration guarantees monotonic convergence [Hunter and Lange, 2004, Wu et al., 2010, Lange, 2016, Zhou et al., 2019] because of this sandwich inequality that directly arises due to the above definition of majorization functions.

$$f(\mathbf{Z}_{t+1}) \leq g(\mathbf{Z}_{t+1}, \mathbf{X}_t) \leq g(\mathbf{X}_t, \mathbf{X}_t) = f(\mathbf{X}_t)$$

The concave-convex procedure to solve the difference of convex (DC) optimization problems is a special case of MM algorithms as follows. For objective functions $f(\mathbf{X})$ which can be written as a difference of convex functions as $f_{\text{vex}}(\mathbf{Z}) + f_{\text{cave}}(\mathbf{Z})$ we have the following majorization function that satisfies the two properties described in the beginning of this subsection.

$$f(\mathbf{Z}) \leq f_{\text{vex}}(\mathbf{Z}) + f_{\text{cave}}(\mathbf{X}) + (\mathbf{Z} - \mathbf{X})^T \nabla f_{\text{cave}}(\mathbf{X}) = g(\mathbf{Z}, \mathbf{X}) \quad (4)$$

where $g(\mathbf{Z}, \mathbf{Z}) = f(\mathbf{Z})$ and $g(\mathbf{Z}, \mathbf{X}) \geq f(\mathbf{Z})$ when $\mathbf{Z} \neq \mathbf{X}$.

Therefore the majorization minimization iterations are

1. Solve $\frac{\partial g(\mathbf{Z}_{t+1}, \mathbf{X}_t)}{\partial \mathbf{Z}_{t+1}} = 0$ for \mathbf{X}_t
2. Set $\mathbf{X}_t = \mathbf{Z}_t$ and continue till convergence.

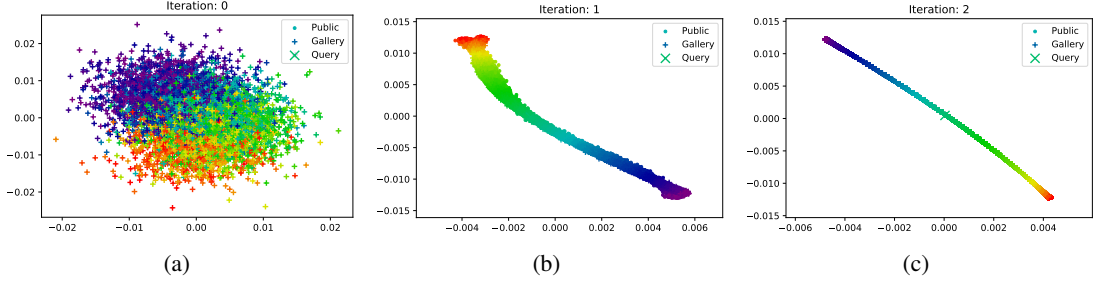


Figure 2: (a-c) Embeddings of our supervised manifold learning technique on CUB (no noise) for 3 iterations with input features extracted from state-of-the-art CGD [Jun et al., 2019] deep image retrieval architecture with ResNet 50 backbone and SG type global descriptors. The colors indicate different class labels. We show that these embeddings preserve information about the class separation and the locality structure required for classification.

This gives the iteration known as the concave-convex procedure.

$$\nabla f_{vex}(\mathbf{Z}_{t+1}) = -\nabla f_{cave}(\mathbf{Z}_t) \quad (5)$$

This can be used to optimize the relaxed version of the supervised manifold learning loss in eqn. 3. This relaxed objective is given below.

$$Tr(\mathbf{Z}^T \mathbf{L}_X \mathbf{Z}) + \lambda Tr(\mathbf{Z}^T \mathbf{S} \mathbf{Q} - \mathbf{v})$$

We first give a first pass solution to optimize this objective function. Using the convex part of the relaxed version of the supervised manifold learning loss given by $f_{vex}(\mathbf{Z}) = Tr(\mathbf{Z}^T \mathbf{L}_X \mathbf{Z}) + \lambda Tr(\mathbf{Z}^T \mathbf{S} \mathbf{Q} - \mathbf{v})$ and concave part of $f_{cave}(\mathbf{Z}) = -\alpha Tr(\mathbf{Z}^T \mathbf{L}_Y \mathbf{Z})$, we can apply the derived iterate in the concave-convex procedure to get

$$\mathbf{Z}_t = \alpha(\mathbf{L}_X)^\dagger [\mathbf{L}_Y \mathbf{Z}_{t-1} - \mathbf{S} \mathbf{Q}] \quad (6)$$

As can be seen, this update does not require a step-size parameter. Secondly, the MM-algorithms of which CCCP is a special case guarantees a monotonic convergence of this update.

4.1.2 Final solution without requiring matrix inverse or a step size parameter

In this section we formulate an efficient monotonically convergent solution for the proposed supervised embedding loss where the update does not require a matrix inverse or a step size parameter. In practice we show that even few iterations of our solution is good enough to give a great embedding.

We denote by $Diag(\mathbf{L}_X)$, a diagonal matrix whose diagonal is the diagonal of \mathbf{L}_X . Now, we can build a majorization function over $Tr(\mathbf{X}^T \mathbf{L}_X \mathbf{X})$, based on the fact that $2Diag(\mathbf{L}_X) - \mathbf{L}_X$ is diagonally dominant. This leads to the following inequality for any matrix \mathbf{M} with real entries and of the same dimension as \mathbf{X} .

$$Tr((\mathbf{X} - \mathbf{M})^T [2Diag(\mathbf{L}_X) - \mathbf{L}_X] (\mathbf{X} - \mathbf{M})) \geq 0$$

as also used in [Vepakomma et al., 2018]. We now get the following majorization inequality over $Tr(\mathbf{X}^T \mathbf{L}_X \mathbf{X})$, by separating it from the above inequality.

$$Tr(\mathbf{X}^T \mathbf{L}_X \mathbf{X}) + \mathbf{b}(\mathbf{Y}) \leq Tr[2\mathbf{X}^T Diag(\mathbf{L}_X) \mathbf{X}] - 2 Tr[\mathbf{X}^T (2Diag(\mathbf{L}_X) - \mathbf{L}_X) \mathbf{M}] = \lambda(\mathbf{X}, \mathbf{M})$$

which is quadratic in \mathbf{X} where, $\mathbf{b}(\mathbf{M}) = Tr(\mathbf{M}^T \mathbf{L}_X \mathbf{M}) - Tr(\mathbf{M}^T 2Diag(\mathbf{L}_X) \mathbf{M})$. Let $h(\mathbf{X}, \mathbf{M}) = \lambda(\mathbf{X}, \mathbf{M}) - \alpha Tr(\mathbf{X}^T \mathbf{L}_Y \mathbf{X})$

This leads to the following bound over our loss function with $const(\mathbf{M})$ being a function that only depends on \mathbf{M} :

$$\mathbf{G}(\mathbf{X}) + const(\mathbf{M}) \leq h(\mathbf{X}, \mathbf{M}) \quad \forall \mathbf{X} \neq \mathbf{M} \\ = h(\mathbf{X}, \mathbf{X}), \text{ when } \mathbf{X} = \mathbf{M}$$

that satisfies the supporting point requirement, and hence $h(\cdot)$ touches the objective function at the current iterate and forms a majorization function. Now the following majorization minimization iteration holds true for an iteration t :

$$\mathbf{X}_{t+1} = \underset{\mathbf{X}}{\operatorname{argmin}} h(\mathbf{X}, \mathbf{M}_t) \text{ and } \mathbf{M}_{t+1} = \mathbf{X}_t$$

It is important to note that these inequalities occur amongst the presence of additive terms, $const(\mathbf{M})$ that are independent of \mathbf{X} unlike a typical majorization-minimization framework and hence, it is a relaxation. The majorization function $h(\mathbf{X}, \mathbf{M}_t)$ can be expressed as a sum of a convex function $e_{vex}(\mathbf{X}) = \lambda(\mathbf{X}, \mathbf{M}_t)$ and a concave function $e_{cave}(\mathbf{X}) = -\alpha Tr(\mathbf{X}^T \mathbf{L}_Y \mathbf{X})$. By the concave-convex formulation, we get the iterative solution by solving for $\nabla e_{vex}(\mathbf{X}_t) = -\nabla e_{cave}(\mathbf{X}_{t-1})$ which gives us

$$\mathbf{X}_t = \frac{\alpha}{2} Diag(\mathbf{L}_X)^\dagger \mathbf{L}_Y \mathbf{X}_{t-1} + \mathbf{M}_t - \frac{1}{2} Diag(\mathbf{L}_X)^\dagger \mathbf{L}_X \mathbf{M}_t$$

and on applying the majorization update over \mathbf{M}_t , we finally get the supervised manifold learning update that does not

require a matrix inversion or a step-size parameter while guaranteeing monotonic convergence.

$$\mathbf{X}_t = \frac{\text{Diag}(\mathbf{L}_X)^\dagger}{2} [\alpha \mathbf{L}_Y - \mathbf{L}_X] \mathbf{X}_{t-1} + \mathbf{X}_{t-1} \quad (7)$$

5 PRIVATIZING THE EMBEDDING

In this section we propose a differentially private mechanism to release the embeddings obtained from our derived supervised manifold learning update in 10. Differential privacy can be achieved by adding noise that is calibrated in relation to the global sensitivity [Dwork et al., 2014] of the query that is being privatized. We first derive a relaxed, yet popular notion of sensitivity called the local sensitivity [Nissim et al., 2007] of our query. We then use it to find a bound on the global sensitivity [Dwork et al., 2014] of our query. Global sensitivity is a much stronger non-relaxed version of sensitivity required for differential privacy. We use the fact that these sensitivities are related as $GS_f = \max_x LS_f(x)$ as a starting point to obtain this upper bound on global sensitivity. We approach the problem by first deriving the local and global sensitivity bounds for one iteration of our update. We then use this to calibrate noise after each iteration of our embedding query. This can be done as every iteration of the query is functionally the same. Global sensitivity is always data independent and only query dependent; thereby allowing for such a noising scheme. We only release the output of the final iteration to the server.

5.1 FINDING THE LOCAL AND GLOBAL SENSITIVITY OF OUR QUERY

We derive a bound on the local sensitivity for the first iteration $f(\mathbf{X}) = \frac{\text{Diag}(\mathbf{L}_X)^\dagger}{2} [\alpha \mathbf{L}_Y - \mathbf{L}_X] \mathbf{Q} + \mathbf{Q}$ where \mathbf{Q} is a random matrix such that $\mathbf{Q}_j \sim \mathcal{N}(\mathbf{0}, \sigma_q^2 \mathbf{I})$. Under all possible cases of keeping $\mathbf{X} \in \mathbb{R}^{n \times k}$ unperturbed except for one neighboring record to produce $\tilde{\mathbf{X}}$, the local sensitivity of the iterate is given by

$$LS_f(\mathbf{X}) = \max_{\tilde{\mathbf{X}}:d(\mathbf{X},\tilde{\mathbf{X}})=1} \|f(\mathbf{X}) - f(\tilde{\mathbf{X}})\|_F \quad (8)$$

Note that we append a row of zeroes to \mathbf{X} and \mathbf{Y} such that the matrix dimensions agree with $\tilde{\mathbf{X}}$ and $\tilde{\mathbf{Y}}$. Let \mathbf{z}_i be the row vector defined by

$$\mathbf{z}_i = [\text{Diag}(\mathbf{L}_X)^\dagger [\alpha \mathbf{L}_Y - \mathbf{L}_X] - \text{Diag}(\mathbf{L}_{\tilde{\mathbf{X}}})^\dagger [\alpha \mathbf{L}_{\tilde{\mathbf{Y}}} - \mathbf{L}_{\tilde{\mathbf{X}}}]]_{i,*} \quad (9)$$

This is the bound on the local sensitivity of our embedding. This help us derive the global sensitivity bound which we need to exactly calibrate the amount of noise that needs to be added to the output of our query to maintain differential privacy.

Theorem 1. Local sensitivity bound of our embedding
With probability $1 - \sum_{\tilde{\mathbf{X}}:d(\mathbf{X},\tilde{\mathbf{X}})=1} \beta$,

$$LS_f(\mathbf{X}) \leq \frac{\sigma_q}{2} \sqrt{-\frac{\ln(\beta) \sum_{i=1}^n \|\mathbf{z}_i\|^4}{\sum_{i=1}^n \|\mathbf{z}_i\|^2} - 2\sqrt{-k \ln(\beta) \sum_{i=1}^n \|\mathbf{z}_i\|^4}}$$

where β is required to satisfy

$$0 < \beta \leq \exp\left(-\frac{4k (\sum_{i=1}^n \|\mathbf{z}_i\|^2)^2}{\sum_{i=1}^n \|\mathbf{z}_i\|^4}\right)$$

Proof. The proof is in Appendix A. \square

We use the local sensitivity bound to obtain the global sensitivity bound.

Corollary 1.1. Global sensitivity bound of our embedding
Let each row in $\mathbf{X}, \tilde{\mathbf{X}}$ be unit norm and each row in $\mathbf{Y}, \tilde{\mathbf{Y}}$ be one-hot encoded. Then with probability $1 - \sum_{\mathbf{X}, \tilde{\mathbf{X}}:d(\mathbf{X},\tilde{\mathbf{X}})=1} \beta$,

$$GS_f \leq \frac{\sigma_q}{2} \sqrt{-\frac{\ln(\beta) (\phi^{\max})^4}{(\phi^{\min})^2} - 2\sqrt{-kn \ln(\beta) (\phi^{\min})^4}} \quad (10)$$

where β is required to satisfy the conditions in Theorem 1 and where ϕ^{\max} and ϕ^{\min} are constants defined in Appendix A.1 such that $\phi^{\min} \leq \|\mathbf{z}_i\| \leq \phi^{\max}$.

Proof. See Appendix A.1. \square

6 EXPERIMENTAL EVALUATION

Datasets: In this section we present experimental results on 2 important image retrieval benchmark datasets of i) Caltech-UCSD Birds-200-2011 (CUB-200-2011) with 200 categories of images and ii) Cars196 with 196 categories of images.

6.1 METHODOLOGY

We use the state of the art image retrieval deep network architecture of CGD [Jun et al., 2019] with ResNet 50 backbone to generate the features for servers dataset concatenated with a publicly shared dataset. We also generate features for client's query concatenated with the same publicly shared dataset. We then privatize the client side features of the concatenated dataset. These are then sent to the server. The server side images are concatenated with publicly shared dataset and a non-private embedding is performed using our

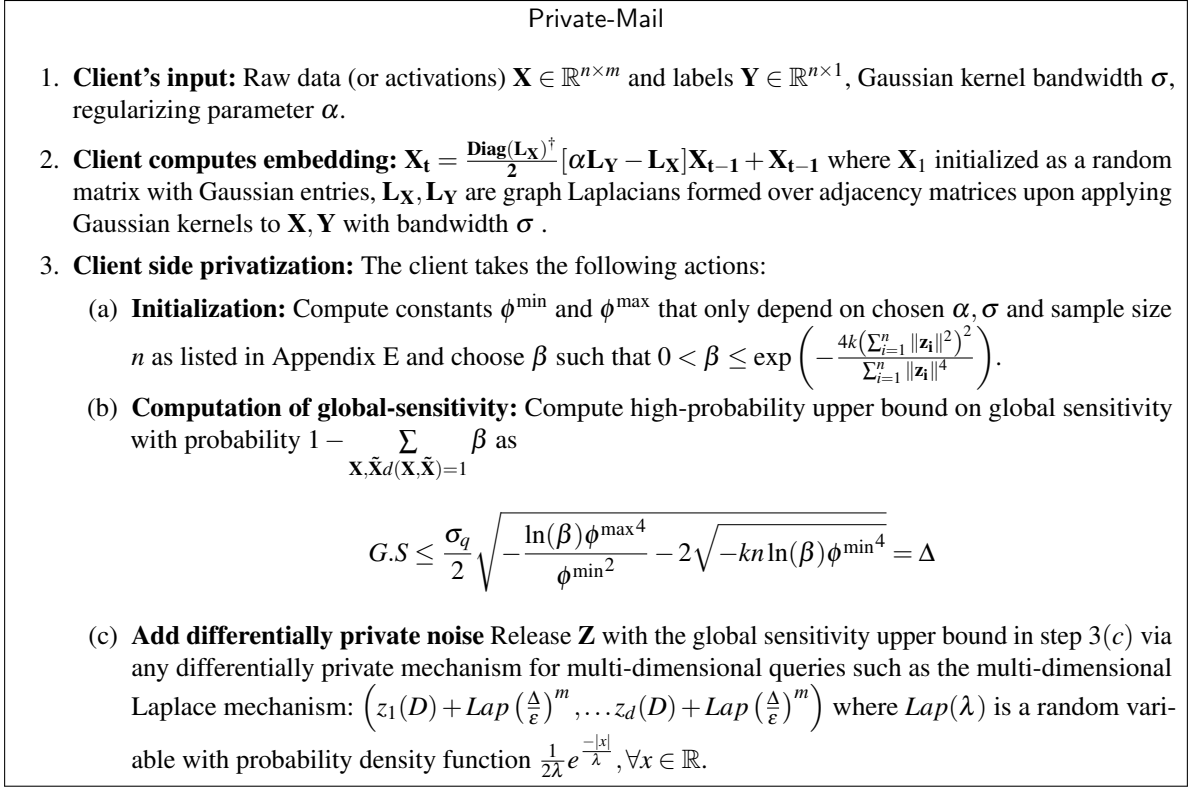


Figure 3: Protocol for the proposed Private-Mail mechanism

supervised manifold learning update in eqn.3. The server's concatenated embeddings and the client's concatenated embeddings are then aligned using the Kabsch-Umeyama algorithm[Umeyama, 1991]. The public dataset is therefore used a common set of anchor points in order to align the embeddings. The query point in the private aligned embedding is used to obtain k nearest matches from the server's images and they are served back to the client. This process is summarized in Figure 1. Algorithm 1 in Appendix F shares the information in greater detail and invokes the proposed differentially private mechanism of PrivateMail in Figure 3.

6.2 METRICS

We compare the important privacy-utility tradeoffs of our mechanism in the Figures 4 (g) and (h). The ϵ 's on the x-axis have been callibrated using the privacy budgeting via the strong composition property given by $\tilde{\epsilon} = \epsilon \sqrt{2k \ln(1/\delta')}$ + $k\epsilon \frac{e^\epsilon - 1}{e^\epsilon + 1}$ and $\tilde{\delta} = k\delta + \delta'$. We privatize the embeddings for 2 iterations of embedding and add the noise after each. We then update the \mathbf{L}_X term in the embedding by recomputing the Laplacian over the private embedding obtained after 2 iterations. This makes the next 2 iterations that we run to be differentially private due to the postprocessing invariance property as the iteration is now functionally independent of the raw dataset \mathbf{X} . We have vizualized the pre- and post-processing embeddings in Figure 4.

References

- Raman Arora and Jalaj Upadhyay. Differentially private graph sparsification and applications. *Advances in neural information processing systems*, 2019.
- Mikhail Belkin and Partha Niyogi. Laplacian eigenmaps for dimensionality reduction and data representation. *Neural computation*, 15(6):1373–1396, 2003.
- Mikhail Belkin and Partha Niyogi. Towards a theoretical foundation for laplacian-based manifold methods. In *International Conference on Computational Learning Theory*, pages 486–500. Springer, 2005.
- Mikhail Belkin and Partha Niyogi. Convergence of laplacian eigenmaps. *Advances in Neural Information Processing Systems*, 19:129, 2007.
- Vishnu Naresh Boddeti. Secure face matching using fully homomorphic encryption. In *2018 IEEE 9th International Conference on Biometrics Theory, Applications and Systems (BTAS)*, pages 1–10. IEEE, 2018.
- Stéphane Boucheron and Maud Thomas. Concentration inequalities for order statistics. *Electronic Communications in Probability*, 17(0), 2012. ISSN 1083-589X. doi: 10.1214/ecp.v17-2210. URL <http://dx.doi.org/10.1214/ECP.v17-2210>.

Algorithm 1: Differentially Private Image Retrieval

input : Client requests k nearest images to its query q , $privIterations$, $PostProcIterations$.

output : Server returns back the k nearest matches back to the client w.r.t its database.

Anchoring with Public Data: Client concatenates its query q with a relevant public dataset \mathcal{P} ;

Feature extraction: Client extracts image-retrieval features for concatenated data $\mathcal{P} \cup q$ from trained ML model ;

Set: $counter = 1$;

for $counter \leq privIterations$ **do**

Run Private-Mail mechanism proposed in Figure 3. and add the prescribed noise in its step 3c.) after every iteration of the embedding in its step 2.;

Set: $counter := counter + 1$;

end

Update: L_X with L_Z by recomputing the Gaussian kernel on $\mathbf{Z} = \mathbf{X}_{counter-1}$;

Set: $counter = 1$;

for $counter \leq PostProcIterations$ **do**

 Only run Step-2 of Private-Mail to update the embeddings ;

Set: $counter := counter + 1$

end

Send: these privatized client embeddings to server;

ServerEmbed: Server embeds $\mathcal{P} \cup ServerImages$;

Align: non-private server embeddings and privatized client embeddings are aligned at server using Kabsch-Umeyama algorithm Umeyama [1991];

Retrieve: Server retrieves k nearest matches w.r.t privatized query embedding in the aligned dataset and serves to the client ;

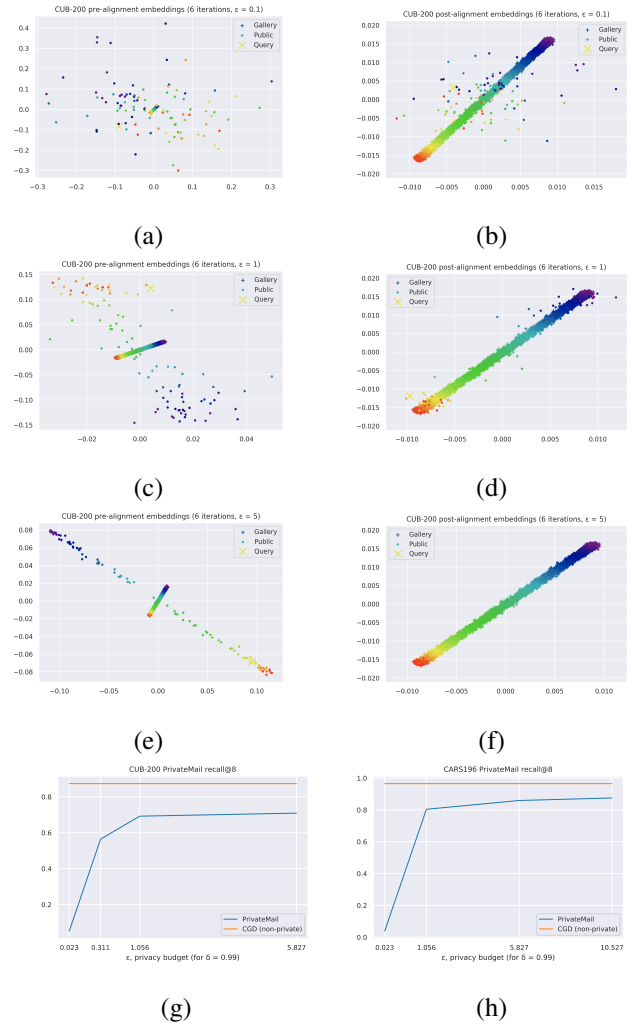


Figure 4: (a-f): Embeddings generated in 6 iterations for CUB-200-2011 data pre- and post- alignment using the Kabsch-Umeyama algorithm [Umeyama, 1991] at varying levels of privacy budget ϵ . We show that alignment improves as less noise is added. (g-h): Image recall@k measurements with $k = 8$ for increasing levels of privacy budget in CUB-200-2011 and Cars196 datasets. We show an increase in retrieval performance as noise decreases with higher ϵ according to the Laplace mechanism. The baseline recall for the CGD [Jun et al., 2019] retrieval is higher at the expense of privacy.

- Stéphane Boucheron, Gábor Lugosi, and Pascal Massart. *Concentration Inequalities: A Nonasymptotic Theory of Independence*. OUP Oxford, 2013.
- Mahawaga Arachchige Pathum Chamikara, Peter Bertok, Ibrahim Khalil, Dongxi Liu, and Seyit Camtepe. Privacy preserving face recognition utilizing differential privacy. *Computers & Security*, 97:101951, 2020.
- Wei Chen, Yu Liu, Weiping Wang, Erwin Bakker, Theodoros Georgiou, Paul Fieguth, Li Liu, and Michael S Lew. Deep image retrieval: A survey. *arXiv preprint arXiv:2101.11282*, 2021.
- Benny Chor, Oded Goldreich, and Eyal Kushilevitz. Private information retrieval. In *Journal of the ACM*, pages 41–50, 1995.
- Anna Choromanska, Krzysztof Choromanski, Geetha Jagannathan, and Claire Monteleoni. Differentially-private learning of low dimensional manifolds. *Theoretical Computer Science*, 620:91–104, 2016.
- Ronald R Coifman and Stéphane Lafon. Diffusion maps. *Applied and computational harmonic analysis*, 21(1):5–30, 2006.
- David L Donoho and Carrie Grimes. Hessian eigenmaps: Locally linear embedding techniques for high-dimensional data. *Proceedings of the National Academy of Sciences*, 100(10):5591–5596, 2003.
- Shiv Ram Dubey. A decade survey of content based image retrieval using deep learning. *arXiv preprint arXiv:2012.00641*, 2020.
- Cynthia Dwork, Aaron Roth, et al. The algorithmic foundations of differential privacy. *Foundations and Trends® in Theoretical Computer Science*, 9(3–4):211–407, 2014.
- Cynthia Dwork, Adam Smith, Thomas Steinke, and Jonathan Ullman. Exposed! a survey of attacks on private data. *Annual Review of Statistics and Its Application*, 4: 61–84, 2017.
- Yousef Elmehdwi, Bharath K Samanthula, and Wei Jiang. Secure k-nearest neighbor query over encrypted data in outsourced environments. In *2014 IEEE 30th International Conference on Data Engineering*, pages 664–675. IEEE, 2014.
- Joshua J Engelsma, Anil K Jain, and Vishnu Naresh Boddeti. Hers: Homomorphically encrypted representation search. *arXiv preprint arXiv:2003.12197*, 2020.
- Simson Garfinkel, John M Abowd, and Christian Martindale. Understanding database reconstruction attacks on public data: These attacks on statistical databases are no longer a theoretical danger. *Queue*, 16(5):28–53, 2018.
- Evarist Giné, Vladimir Koltchinskii, et al. Empirical graph laplacian approximation of laplace–beltrami operators: Large sample results. In *High dimensional probability*, pages 238–259. Institute of Mathematical Statistics, 2006.
- Chaoyang He, Songze Li, Jinhyun So, Mi Zhang, Hongyi Wang, Xiaoyang Wang, Praneeth Vepakomma, Abhishek Singh, Hang Qiu, Li Shen, et al. Fedml: A research library and benchmark for federated machine learning. *arXiv preprint arXiv:2007.13518*, 2020.
- David R Hunter and Kenneth Lange. A tutorial on mm algorithms. *The American Statistician*, 58(1):30–37, 2004.
- Peter W Jones, Mauro Maggioni, and Raanan Schul. Manifold parametrizations by eigenfunctions of the laplacian and heat kernels. *Proceedings of the National Academy of Sciences*, 105(6):1803–1808, 2008.
- HeeJae Jun, ByungSoo Ko, Youngjoon Kim, Insik Kim, and Jongtaek Kim. Combination of multiple global descriptors for image retrieval. *arXiv preprint arXiv:1903.10663*, 2019.
- Kenneth Lange. *MM optimization algorithms*. SIAM, 2016.
- Xinyu Lei, Alex X Liu, Rui Li, and Guan-Hua Tu. Seceqp: A secure and efficient scheme for sknn query problem over encrypted geodata on cloud. In *2019 IEEE 35th International Conference on Data Engineering (ICDE)*, pages 662–673. IEEE, 2019.
- Zheng Li and Yang Zhang. Label-leaks: Membership inference attack with label. *arXiv preprint arXiv:2007.15528*, 2020.
- Yusuke Matsui, Takuma Yamaguchi, and Zheng Wang. Cvpr2020 tutorial on image retrieval in the wild. https://matsui528.github.io/cvpr2020_tutorial_retrieval/, 2020.
- Kobbi Nissim, Sofya Raskhodnikova, and Adam Smith. Smooth sensitivity and sampling in private data analysis. In *Proceedings of the thirty-ninth annual ACM symposium on Theory of computing*, pages 75–84, 2007.
- Jagarlamudi Shashank, Palivela Kowshik, Kannan Sri-nathan, and CV Jawahar. Private content based image retrieval. In *2008 IEEE Conference on Computer Vision and Pattern Recognition*, pages 1–8. IEEE, 2008.
- Yi Shi, Kemal Davaslioglu, and Yalin E Sagduyu. Over-the-air membership inference attacks as privacy threats for deep learning-based wireless signal classifiers. In *Proceedings of the 2nd ACM Workshop on Wireless Security and Machine Learning*, pages 61–66, 2020.
- Reza Shokri, Marco Stronati, Congzheng Song, and Vitaly Shmatikov. Membership inference attacks against machine learning models. In *2017 IEEE Symposium on Security and Privacy (SP)*, pages 3–18. IEEE, 2017.

- Liwei Song, Reza Shokri, and Prateek Mittal. Membership inference attacks against adversarially robust deep learning models. In *2019 IEEE Security and Privacy Workshops (SPW)*, pages 50–56. IEEE, 2019.
- Julian Steil, Inken Hagedstedt, Michael Xuelin Huang, and Andreas Bulling. Privacy-aware eye tracking using differential privacy. In *Proceedings of the 11th ACM Symposium on Eye Tracking Research & Applications*, pages 1–9, 2019.
- Stacey Truex, Ling Liu, Mehmet Emre Gursoy, Lei Yu, and Wenqi Wei. Towards demystifying membership inference attacks. *arXiv preprint arXiv:1807.09173*, 2018.
- Matthew Turk and Alex Pentland. Eigenfaces for recognition. *Journal of cognitive neuroscience*, 3(1):71–86, 1991.
- Shinji Umeyama. Least-squares estimation of transformation parameters between two point patterns. *IEEE Computer Architecture Letters*, 13(04):376–380, 1991.
- Laurens Van der Maaten and Geoffrey Hinton. Visualizing data using t-sne. *Journal of machine learning research*, 9(11), 2008.
- Praneeth Vepakomma and Ahmed Elgammal. A fast algorithm for manifold learning by posing it as a symmetric diagonally dominant linear system. *Applied and Computational Harmonic Analysis*, 40(3):622–628, 2016.
- Praneeth Vepakomma, Chetan Tonde, Ahmed Elgammal, et al. Supervised dimensionality reduction via distance correlation maximization. *Electronic Journal of Statistics*, 12(1):960–984, 2018.
- Elif Vural and Christine Guillemot. A study of the classification of low-dimensional data with supervised manifold learning. *J. Mach. Learn. Res.*, 18(1):5741–5795, 2017.
- Tong Tong Wu, Kenneth Lange, et al. The mm alternative to em. *Statistical Science*, 25(4):492–505, 2010.
- Zhihua Xia, Yi Zhu, Xingming Sun, Zhan Qin, and Kui Ren. Towards privacy-preserving content-based image retrieval in cloud computing. *IEEE Transactions on Cloud Computing*, 6(1):276–286, 2015.
- Bin Yao, Feifei Li, and Xiaokui Xiao. Secure nearest neighbor revisited. In *2013 IEEE 29th international conference on data engineering (ICDE)*, pages 733–744. IEEE, 2013.
- Hua Zhou, Liuyi Hu, Jin Zhou, and Kenneth Lange. Mm algorithms for variance components models. *Journal of Computational and Graphical Statistics*, 28(2):350–361, 2019.
- Wengang Zhou, Houqiang Li, and Qi Tian. Recent advance in content-based image retrieval: A literature survey. *arXiv preprint arXiv:1706.06064*, 2017.

Appendices

A PROOF OF THEOREM 1

Proof. The square of the Frobenius norm in equation 8 is given by

$$\begin{aligned} \|f(\mathbf{X}) - f(\tilde{\mathbf{X}})\|_F^2 &= \left\| \frac{\text{Diag}(\mathbf{L}_X)^\dagger [\alpha \mathbf{L}_Y - \mathbf{L}_X] - \text{Diag}(\mathbf{L}_{\tilde{X}})^\dagger [\alpha \mathbf{L}_{\tilde{Y}} - \mathbf{L}_{\tilde{X}}]}{2} \mathbf{Q} \right\|_F^2 \\ &= \frac{1}{4} \sum_{i=1}^n \sum_{j=1}^k \langle \mathbf{z}_i, \mathbf{Q}_j \rangle^2 \end{aligned} \quad (11)$$

By the affine transformation property of multivariate Gaussians,

$$\begin{aligned} \langle \mathbf{z}_i, \mathbf{Q}_j \rangle &\sim \mathcal{N}(0, \sigma_q^2 \mathbf{z}_i^\top \mathbf{I} \mathbf{z}_i) = \mathcal{N}(0, \sigma_q^2 \|\mathbf{z}_i\|^2) \\ \sum_{j=1}^k \langle \mathbf{z}_i, \mathbf{Q}_j \rangle^2 &\sim \Gamma\left(\frac{k}{2}, 2\sigma_q^2 \|\mathbf{z}_i\|^2\right) \end{aligned}$$

The sum of gamma distributions can be approximated by the Welch–Satterthwaite equation,

$$\begin{aligned} \sum_i \Gamma(k_i, \theta_i) &\sim \Gamma(k_{\text{sum}}, \theta_{\text{sum}}) \\ k_{\text{sum}} &= \frac{(\sum_i \theta_i k_i)^2}{\sum_i \theta_i^2 k_i} \quad \theta_{\text{sum}} = \frac{\sum_i \theta_i k_i}{k_{\text{sum}}} \end{aligned}$$

Thus,

$$\begin{aligned} \frac{1}{4} \sum_{i=1}^n \sum_{j=1}^k \langle \mathbf{z}_i, \mathbf{Q}_j \rangle^2 &\sim \frac{1}{4} \Gamma\left(\frac{(\sum_{i=1}^n 2\sigma_q^2 \|\mathbf{z}_i\|^2 \frac{k}{2})^2}{\sum_{i=1}^n (2\sigma_q^2 \|\mathbf{z}_i\|^2)^2 \frac{k}{2}}, \frac{\sum_{i=1}^n (2\sigma_q^2 \|\mathbf{z}_i\|^2)^2 \frac{k}{2}}{\sum_{i=1}^n 2\sigma_q^2 \|\mathbf{z}_i\|^2 \frac{k}{2}}\right) \\ &= \Gamma\left(\frac{k (\sum_{i=1}^n \|\mathbf{z}_i\|^2)^2}{2 \sum_{i=1}^n \|\mathbf{z}_i\|^4}, \frac{\sigma_q^2 \sum_{i=1}^n \|\mathbf{z}_i\|^4}{2 \sum_{i=1}^n \|\mathbf{z}_i\|^2}\right) \end{aligned} \quad (12)$$

A gamma random variable Y with shape p and scale parameter c is sub-gamma on the right tail with variance factor pc^2 and scale factor c [Boucheron and Thomas, 2012]. As discussed by Boucheron et al. [2013], the sub-gamma property is then characterized by the following tail conditions: for every $t > 0$,

$$\begin{aligned} \mathbb{P}(Y > t) &\leq \exp\left(-\frac{pc^2}{c^2} h\left(\frac{ct}{pc^2}\right)\right) \\ &= \exp\left(-ph\left(\frac{t}{pc}\right)\right) \end{aligned} \quad (13)$$

where $h(u) = 1 + u - \sqrt{1 + 2u}$ for $u > 0$. Applying this to equation (12), we have

$$\begin{aligned} \mathbb{P}(\|f(\mathbf{X}) - f(\tilde{\mathbf{X}})\|_F > \sqrt{t}) &= \mathbb{P}(\|f(\mathbf{X}) - f(\tilde{\mathbf{X}})\|_F^2 > t) \\ &\leq \exp\left(-\frac{k (\sum_{i=1}^n \|\mathbf{z}_i\|^2)^2}{2 \sum_{i=1}^n \|\mathbf{z}_i\|^4} \left[1 + \frac{4t}{k \sigma_q^2 \sum_{i=1}^n \|\mathbf{z}_i\|^2} - \sqrt{1 + \frac{8t}{k \sigma_q^2 \sum_{i=1}^n \|\mathbf{z}_i\|^2}}\right]\right) \\ &= \exp\left(\frac{k (\sum_{i=1}^n \|\mathbf{z}_i\|^2)^2}{2 \sum_{i=1}^n \|\mathbf{z}_i\|^4} \sqrt{1 + \frac{8t}{k \sigma_q^2 \sum_{i=1}^n \|\mathbf{z}_i\|^2}} - \frac{k (\sum_{i=1}^n \|\mathbf{z}_i\|^2)^2}{2 \sum_{i=1}^n \|\mathbf{z}_i\|^4} - \frac{2t \sum_{i=1}^n \|\mathbf{z}_i\|^2}{\sigma_q^2 \sum_{i=1}^n \|\mathbf{z}_i\|^4}\right) \\ &\leq \beta \end{aligned} \quad (14)$$

For very small β , we can conclude with high probability $1 - \beta$ that $\|f(\mathbf{X}) - f(\tilde{\mathbf{X}})\| \leq \sqrt{t}$. The tightest such bound is thus given by

$$\begin{aligned} \min \quad & \sqrt{t} \\ \text{s.t.} \quad & \exp\left(\frac{k(\sum_{i=1}^n \|\mathbf{z}_i\|^2)^2}{2\sum_{i=1}^n \|\mathbf{z}_i\|^4} \sqrt{1 + \frac{8t}{k\sigma_q^2 \sum_{i=1}^n \|\mathbf{z}_i\|^2}} - \frac{k(\sum_{i=1}^n \|\mathbf{z}_i\|^2)^2}{2\sum_{i=1}^n \|\mathbf{z}_i\|^4} - \frac{2t\sum_{i=1}^n \|\mathbf{z}_i\|^2}{\sigma_q^2 \sum_{i=1}^n \|\mathbf{z}_i\|^4}\right) = \beta \\ & t \geq 0 \end{aligned} \tag{15}$$

The condition $t \geq 0$ must hold since $\|f(\mathbf{X}) - f(\tilde{\mathbf{X}})\|_F$ is always nonnegative. Further simplifying, we obtain the quadratic constraint

$$\begin{aligned} \exp\left(\frac{k(\sum_{i=1}^n \|\mathbf{z}_i\|^2)^2}{2\sum_{i=1}^n \|\mathbf{z}_i\|^4} \sqrt{1 + \frac{8t}{k\sigma_q^2 \sum_{i=1}^n \|\mathbf{z}_i\|^2}} - \frac{k(\sum_{i=1}^n \|\mathbf{z}_i\|^2)^2}{2\sum_{i=1}^n \|\mathbf{z}_i\|^4} - \frac{2t\sum_{i=1}^n \|\mathbf{z}_i\|^2}{\sigma_q^2 \sum_{i=1}^n \|\mathbf{z}_i\|^4}\right) &= \beta \\ \frac{k(\sum_{i=1}^n \|\mathbf{z}_i\|^2)^2}{2\sum_{i=1}^n \|\mathbf{z}_i\|^4} \sqrt{1 + \frac{8t}{k\sigma_q^2 \sum_{i=1}^n \|\mathbf{z}_i\|^2}} - \frac{k(\sum_{i=1}^n \|\mathbf{z}_i\|^2)^2}{2\sum_{i=1}^n \|\mathbf{z}_i\|^4} - \frac{2t\sum_{i=1}^n \|\mathbf{z}_i\|^2}{\sigma_q^2 \sum_{i=1}^n \|\mathbf{z}_i\|^4} &= \ln(\beta) \\ a\sqrt{1+bt} - a - ct = \ln(\beta) \quad \text{where } a = \frac{k(\sum_{i=1}^n \|\mathbf{z}_i\|^2)^2}{2\sum_{i=1}^n \|\mathbf{z}_i\|^4}, b = \frac{8}{k\sigma_q^2 \sum_{i=1}^n \|\mathbf{z}_i\|^2}, \text{ and } c = \frac{2\sum_{i=1}^n \|\mathbf{z}_i\|^2}{\sigma_q^2 \sum_{i=1}^n \|\mathbf{z}_i\|^4} \\ a\sqrt{1+bt} &= \ln(\beta) + a + ct \\ a^2(1+bt) &= (\ln(\beta) + a)^2 + 2c(\ln(\beta) + a)t + c^2t^2 \\ 0 &= c^2t^2 + [2c(\ln(\beta) + a) - a^2b]t + \ln^2(\beta) + 2\ln(\beta)a \\ 0 &= \hat{a}t^2 + \hat{b}t + \hat{c} \quad \text{where } \hat{a} = c^2, \hat{b} = 2c(\ln(\beta) + a) - a^2b, \text{ and } \hat{c} = \ln^2(\beta) + 2\ln(\beta)a \\ \implies t &= \frac{-\hat{b} \pm \sqrt{\hat{b}^2 - 4\hat{a}\hat{c}}}{2\hat{a}} \end{aligned}$$

Plugging the constant values back in, we have

$$\begin{aligned} \hat{a} = c^2 &= \left(\frac{2\sum_{i=1}^n \|\mathbf{z}_i\|^2}{\sigma_q^2 \sum_{i=1}^n \|\mathbf{z}_i\|^4}\right)^2 = \frac{4(\sum_{i=1}^n \|\mathbf{z}_i\|^2)^2}{\sigma_q^4 (\sum_{i=1}^n \|\mathbf{z}_i\|^4)^2} \\ \hat{b} = 2c(\ln(\beta) + a) - a^2b &= \frac{4\sum_{i=1}^n \|\mathbf{z}_i\|^2}{\sigma_q^2 \sum_{i=1}^n \|\mathbf{z}_i\|^4} \left(\ln(\beta) + \frac{k(\sum_{i=1}^n \|\mathbf{z}_i\|^2)^2}{2\sum_{i=1}^n \|\mathbf{z}_i\|^4}\right) - \left(\frac{k(\sum_{i=1}^n \|\mathbf{z}_i\|^2)^2}{2\sum_{i=1}^n \|\mathbf{z}_i\|^4}\right)^2 \frac{8}{k\sigma_q^2 \sum_{i=1}^n \|\mathbf{z}_i\|^2} \\ &= \frac{4\ln(\beta)\sum_{i=1}^n \|\mathbf{z}_i\|^2}{\sigma_q^2 \sum_{i=1}^n \|\mathbf{z}_i\|^4} + \frac{2k(\sum_{i=1}^n \|\mathbf{z}_i\|^2)^3}{\sigma_q^2 (\sum_{i=1}^n \|\mathbf{z}_i\|^4)^2} - \frac{2k(\sum_{i=1}^n \|\mathbf{z}_i\|^2)^3}{\sigma_q^2 (\sum_{i=1}^n \|\mathbf{z}_i\|^4)^2} \\ &= \frac{4\ln(\beta)\sum_{i=1}^n \|\mathbf{z}_i\|^2}{\sigma_q^2 \sum_{i=1}^n \|\mathbf{z}_i\|^4} \\ \hat{c} = \ln^2(\beta) + 2\ln(\beta)a &= \ln^2(\beta) + \frac{k\ln(\beta)(\sum_{i=1}^n \|\mathbf{z}_i\|^2)^2}{\sum_{i=1}^n \|\mathbf{z}_i\|^4} \end{aligned}$$

We now solve for t^* ,

$$\begin{aligned}
t^* &= \frac{-\frac{4\ln(\beta)\sum_{i=1}^n\|\mathbf{z}_i\|^2}{\sigma_q^2\sum_{i=1}^n\|\mathbf{z}_i\|^4} \pm \sqrt{\left(\frac{4\ln(\beta)\sum_{i=1}^n\|\mathbf{z}_i\|^2}{\sigma_q^2\sum_{i=1}^n\|\mathbf{z}_i\|^4}\right)^2 - 4 \cdot \frac{4(\sum_{i=1}^n\|\mathbf{z}_i\|^2)^2}{\sigma_q^4(\sum_{i=1}^n\|\mathbf{z}_i\|^4)^2} \left(\ln^2(\beta) + \frac{k\ln(\beta)(\sum_{i=1}^n\|\mathbf{z}_i\|^2)^2}{\sum_{i=1}^n\|\mathbf{z}_i\|^4}\right)}}{2 \cdot \frac{4(\sum_{i=1}^n\|\mathbf{z}_i\|^2)^2}{\sigma_q^4(\sum_{i=1}^n\|\mathbf{z}_i\|^4)^2}} \\
&= \frac{-\frac{4\ln(\beta)\sum_{i=1}^n\|\mathbf{z}_i\|^2}{\sigma_q^2\sum_{i=1}^n\|\mathbf{z}_i\|^4} \pm \sqrt{\frac{16\ln^2(\beta)(\sum_{i=1}^n\|\mathbf{z}_i\|^2)^2}{\sigma_q^4(\sum_{i=1}^n\|\mathbf{z}_i\|^4)^2} - \frac{16\ln^2(\beta)(\sum_{i=1}^n\|\mathbf{z}_i\|^2)^2}{\sigma_q^4(\sum_{i=1}^n\|\mathbf{z}_i\|^4)^2} - \frac{16k\ln(\beta)(\sum_{i=1}^n\|\mathbf{z}_i\|^2)^4}{\sigma_q^4(\sum_{i=1}^n\|\mathbf{z}_i\|^4)^3}}}{\frac{8(\sum_{i=1}^n\|\mathbf{z}_i\|^2)^2}{\sigma_q^4(\sum_{i=1}^n\|\mathbf{z}_i\|^4)^2}} \\
&= \frac{-\frac{4\ln(\beta)\sum_{i=1}^n\|\mathbf{z}_i\|^2}{\sigma_q^2\sum_{i=1}^n\|\mathbf{z}_i\|^4} \pm \frac{4(\sum_{i=1}^n\|\mathbf{z}_i\|^2)^2}{\sigma_q^2\sum_{i=1}^n\|\mathbf{z}_i\|^4} \sqrt{-\frac{k\ln(\beta)}{\sum_{i=1}^n\|\mathbf{z}_i\|^4}}}{\frac{8(\sum_{i=1}^n\|\mathbf{z}_i\|^2)^2}{\sigma_q^4(\sum_{i=1}^n\|\mathbf{z}_i\|^4)^2}} \\
&= -\frac{\ln(\beta)\sum_{i=1}^n\|\mathbf{z}_i\|^2 \pm (\sum_{i=1}^n\|\mathbf{z}_i\|^2)^2 \sqrt{-\frac{k\ln(\beta)}{\sum_{i=1}^n\|\mathbf{z}_i\|^4}}}{\frac{2(\sum_{i=1}^n\|\mathbf{z}_i\|^2)^2}{\sigma_q^2\sum_{i=1}^n\|\mathbf{z}_i\|^4}} \\
&= -\frac{\sigma_q^2\ln(\beta)\sum_{i=1}^n\|\mathbf{z}_i\|^4}{2\sum_{i=1}^n\|\mathbf{z}_i\|^2} \pm \frac{\sigma_q^2\sum_{i=1}^n\|\mathbf{z}_i\|^4}{2} \sqrt{-\frac{k\ln(\beta)}{\sum_{i=1}^n\|\mathbf{z}_i\|^4}} \\
&= \frac{\sigma_q^2}{2} \left[-\frac{\ln(\beta)\sum_{i=1}^n\|\mathbf{z}_i\|^4}{2\sum_{i=1}^n\|\mathbf{z}_i\|^2} \pm \sqrt{-k\ln(\beta)\sum_{i=1}^n\|\mathbf{z}_i\|^4} \right]
\end{aligned}$$

Since $0 < \beta < 1$, then $\ln(\beta) < 0$. Therefore, we may choose t^* to be the smaller solution

$$t^* = \frac{\sigma_q^2}{2} \left[-\frac{\ln(\beta)\sum_{i=1}^n\|\mathbf{z}_i\|^4}{2\sum_{i=1}^n\|\mathbf{z}_i\|^2} - \sqrt{-k\ln(\beta)\sum_{i=1}^n\|\mathbf{z}_i\|^4} \right] \leq \frac{\sigma_q^2}{2} \left[-\frac{\ln(\beta)\sum_{i=1}^n\|\mathbf{z}_i\|^4}{2\sum_{i=1}^n\|\mathbf{z}_i\|^2} + \sqrt{-k\ln(\beta)\sum_{i=1}^n\|\mathbf{z}_i\|^4} \right] \quad (16)$$

It remains to check the conditions under which this solution satisfies $t^* \geq 0$.

$$\begin{aligned}
t^* &= \frac{\sigma_q^2}{2} \left[-\frac{\ln(\beta)\sum_{i=1}^n\|\mathbf{z}_i\|^4}{2\sum_{i=1}^n\|\mathbf{z}_i\|^2} - \sqrt{-k\ln(\beta)\sum_{i=1}^n\|\mathbf{z}_i\|^4} \right] \geq 0 \\
&\quad -\frac{\ln(\beta)\sum_{i=1}^n\|\mathbf{z}_i\|^4}{2\sum_{i=1}^n\|\mathbf{z}_i\|^2} - \sqrt{-k\ln(\beta)\sum_{i=1}^n\|\mathbf{z}_i\|^4} \geq 0 \\
&\quad -\sqrt{-k\ln(\beta)\sum_{i=1}^n\|\mathbf{z}_i\|^4} \geq \frac{\ln(\beta)\sum_{i=1}^n\|\mathbf{z}_i\|^4}{2\sum_{i=1}^n\|\mathbf{z}_i\|^2} \\
&\quad -k\ln(\beta)\sum_{i=1}^n\|\mathbf{z}_i\|^4 \leq \frac{\ln^2(\beta)(\sum_{i=1}^n\|\mathbf{z}_i\|^4)^2}{4(\sum_{i=1}^n\|\mathbf{z}_i\|^2)^2} \\
&\quad -k \geq \frac{\ln(\beta)\sum_{i=1}^n\|\mathbf{z}_i\|^4}{4(\sum_{i=1}^n\|\mathbf{z}_i\|^2)^2} \\
&\quad -\frac{4k(\sum_{i=1}^n\|\mathbf{z}_i\|^2)^2}{\sum_{i=1}^n\|\mathbf{z}_i\|^4} \geq \ln(\beta) \\
&\quad \exp\left(-\frac{4k(\sum_{i=1}^n\|\mathbf{z}_i\|^2)^2}{\sum_{i=1}^n\|\mathbf{z}_i\|^4}\right) \geq \beta
\end{aligned}$$

Thus, with probability $1 - \beta$,

$$\begin{aligned}
\|f(\mathbf{X}) - f(\tilde{\mathbf{X}})\|_F &\leq \sqrt{t^*} \\
&= \sqrt{\frac{\sigma_q^2}{2} \left[-\frac{\ln(\beta) \sum_{i=1}^n \|\mathbf{z}_i\|^4}{2 \sum_{i=1}^n \|\mathbf{z}_i\|^2} - \sqrt{-k \ln(\beta) \sum_{i=1}^n \|\mathbf{z}_i\|^4} \right]} \\
&= \frac{\sigma_q}{2} \sqrt{-\frac{\ln(\beta) \sum_{i=1}^n \|\mathbf{z}_i\|^4}{\sum_{i=1}^n \|\mathbf{z}_i\|^2} - 2 \sqrt{-k \ln(\beta) \sum_{i=1}^n \|\mathbf{z}_i\|^4}}
\end{aligned} \tag{17}$$

where

$$0 < \beta \leq \exp\left(-\frac{4k(\sum_{i=1}^n \|\mathbf{z}_i\|^2)^2}{\sum_{i=1}^n \|\mathbf{z}_i\|^4}\right) \tag{18}$$

By the union bound, we have

$$\begin{aligned}
\mathbb{P}(LS_f(\mathbf{X}) > \sqrt{t^*}) &= \mathbb{P}\left(\max_{\tilde{\mathbf{X}}:d(\mathbf{X},\tilde{\mathbf{X}})=1} \|f(\mathbf{X}) - f(\tilde{\mathbf{X}})\|_F > \sqrt{t^*}\right) \\
&= \mathbb{P}\left(\bigcup_{\tilde{\mathbf{X}}:d(\mathbf{X},\tilde{\mathbf{X}})=1} \{\|f(\mathbf{X}) - f(\tilde{\mathbf{X}})\|_F > \sqrt{t^*}\}\right) \\
&\leq \sum_{\tilde{\mathbf{X}}:d(\mathbf{X},\tilde{\mathbf{X}})=1} \mathbb{P}\left(\|f(\mathbf{X}) - f(\tilde{\mathbf{X}})\|_F > \sqrt{t^*}\right) \\
&\leq \sum_{\tilde{\mathbf{X}}:d(\mathbf{X},\tilde{\mathbf{X}})=1} \beta
\end{aligned} \tag{19}$$

Then $LS_f(\mathbf{X}) \leq \frac{\sigma_q}{2} \sqrt{-\frac{\ln(\beta) \sum_{i=1}^n \|\mathbf{z}_i\|^4}{\sum_{i=1}^n \|\mathbf{z}_i\|^2} - 2 \sqrt{-k \ln(\beta) \sum_{i=1}^n \|\mathbf{z}_i\|^4}}$ with probability $1 - \sum_{\tilde{\mathbf{X}}:d(\mathbf{X},\tilde{\mathbf{X}})=1} \beta$. \square

A.1 PROOF OF COROLLARY 1.1

By the union bound, we have

$$\begin{aligned}
\mathbb{P}(GS_f > t) &= \mathbb{P}\left(\max_{\tilde{\mathbf{X}}} LS_f(\mathbf{X}) > t\right) \\
&= \mathbb{P}\left(\bigcup_{\tilde{\mathbf{X}}} \{LS_f(\mathbf{X}) > t\}\right) \\
&\leq \sum_{\tilde{\mathbf{X}}} \mathbb{P}(LS_f(\mathbf{X}) > t) \\
&\leq \sum_{\tilde{\mathbf{X}}} \sum_{\tilde{\mathbf{X}}:d(\mathbf{X},\tilde{\mathbf{X}})=1} \beta
\end{aligned} \tag{20}$$

Plugging in the right hand side of the inequality of Theorem 1 for t , we have

$$GS_f \leq \min_{\mathbf{X}, \tilde{\mathbf{X}}} \left\{ \frac{\sigma_q}{2} \sqrt{-\frac{\ln(\beta) \sum_{i=1}^n \|\mathbf{z}_i\|^4}{\sum_{i=1}^n \|\mathbf{z}_i\|^2} - 2 \sqrt{-k \ln(\beta) \sum_{i=1}^n \|\mathbf{z}_i\|^4}} \right\} \tag{21}$$

with probability $1 - \sum_{\tilde{\mathbf{X}}:d(\mathbf{X},\tilde{\mathbf{X}})=1} \beta$ with β satisfying the aforementioned conditions. Note that this bound includes \mathbf{z}_i , which is a function of \mathbf{X} and $\tilde{\mathbf{X}}$. However, global sensitivity is a constant by definition, so we take a minimum over all possible \mathbf{X} , $\tilde{\mathbf{X}}$, as the bound holds for all possible neighboring datasets.

As defined in Theorem 1, $\|\mathbf{z}_i\|$ is a function of \mathbf{X} and $\tilde{\mathbf{X}}$, where the laplacian matrix \mathbf{L}_X is defined by

$$\mathbf{L}_X = \text{Diag} \left(\sum_{i=1}^{n+1} \mathbf{W}^X_{i,1}, \dots, \sum_{i=1}^{n+1} \mathbf{W}^X_{i,n+1} \right) - \mathbf{W}^X \quad (22)$$

and where \mathbf{W}^X is the gaussian kernel given by

$$\mathbf{W}^X_{i,j} = \exp \left(-\frac{\|\mathbf{X}^T_i - \mathbf{X}^T_j\|^2}{2\sigma^2} \right) \quad (23)$$

for some user-defined σ . $\mathbf{L}_{\tilde{X}}$, \mathbf{L}_Y , and $\mathbf{L}_{\tilde{Y}}$ are defined similarly for $\tilde{\mathbf{X}}$, \mathbf{Y} , and $\tilde{\mathbf{Y}}$ respectively. If $\phi^{\min} \leq \|\mathbf{z}_i\| \leq \phi^{\max}$, then by Theorem 1,

$$LS_f(\mathbf{X}) \leq \frac{\sigma_q}{2} \sqrt{-\frac{\ln(\beta) \sum_{i=1}^n \|\mathbf{z}_i\|^4}{\sum_{i=1}^n \|\mathbf{z}_i\|^2} - 2} \sqrt{-k \ln(\beta) \sum_{i=1}^n \|\mathbf{z}_i\|^4} \leq \frac{\sigma_q}{2} \sqrt{-\frac{\ln(\beta)(\phi^{\max})^4}{(\phi^{\min})^2} - 2} \sqrt{-kn \ln(\beta)(\phi^{\min})^4} \quad (24)$$

with probability $1 - \sum_{\tilde{\mathbf{X}}:d(\mathbf{X},\tilde{\mathbf{X}})=1} \beta$. We now derive such bounds for ϕ^{\min} and ϕ^{\max} . Expanding equation (9),

$$\begin{aligned} \|\mathbf{z}_i\| &= \mathbf{z}_i^T \mathbf{z}_i \\ &= \sum_{j=1}^{n+1} [\text{Diag}(\mathbf{L}_X)^\dagger [\alpha \mathbf{L}_Y - \mathbf{L}_X] - \text{Diag}(\mathbf{L}_{\tilde{X}})^\dagger [\alpha \mathbf{L}_{\tilde{Y}} - \mathbf{L}_{\tilde{X}}]]_{i,j}^2 \\ &= \sum_{j=1}^{n+1} \left([\text{Diag}(\mathbf{L}_X)^\dagger [\alpha \mathbf{L}_Y - \mathbf{L}_X]]_{i,j} - [\text{Diag}(\mathbf{L}_{\tilde{X}})^\dagger [\alpha \mathbf{L}_{\tilde{Y}} - \mathbf{L}_{\tilde{X}}]]_{i,j} \right)^2 \\ &= \sum_{j=1}^{n+1} \left([\text{Diag}(\mathbf{L}_X)^\dagger [\alpha \mathbf{L}_Y - \mathbf{L}_X]]_{i,j}^2 + [\text{Diag}(\mathbf{L}_{\tilde{X}})^\dagger [\alpha \mathbf{L}_{\tilde{Y}} - \mathbf{L}_{\tilde{X}}]]_{i,j}^2 - 2 [\text{Diag}(\mathbf{L}_X)^\dagger [\alpha \mathbf{L}_Y - \mathbf{L}_X]]_{i,j} [\text{Diag}(\mathbf{L}_{\tilde{X}})^\dagger [\alpha \mathbf{L}_{\tilde{Y}} - \mathbf{L}_{\tilde{X}}]]_{i,j} \right) \end{aligned}$$

Since the off-diagonal entries of $\text{Diag}(\mathbf{L}_X)$ and $\text{Diag}(\mathbf{L}_{\tilde{X}})$ are zero, we have

$$\begin{aligned} [\text{Diag}(\mathbf{L}_X)^\dagger [\alpha \mathbf{L}_Y - \mathbf{L}_X]]_{i,j} &= \sum_{k=1}^n \text{Diag}(\mathbf{L}_X)^\dagger_{i,k} [\alpha \mathbf{L}_Y - \mathbf{L}_X]_{k,j} = \text{Diag}(\mathbf{L}_X)^\dagger_{i,i} [\alpha \mathbf{L}_Y - \mathbf{L}_X]_{i,j} = \frac{\alpha \mathbf{L}_{Yi,j} - \mathbf{L}_{Xi,j}}{\text{Diag}(\mathbf{L}_X)_{i,i}} \\ [\text{Diag}(\mathbf{L}_{\tilde{X}})^\dagger [\alpha \mathbf{L}_{\tilde{Y}} - \mathbf{L}_{\tilde{X}}]]_{i,j} &= \sum_{k=1}^n \text{Diag}(\mathbf{L}_{\tilde{X}})^\dagger_{i,k} [\alpha \mathbf{L}_{\tilde{Y}} - \mathbf{L}_{\tilde{X}}]_{k,j} = \text{Diag}(\mathbf{L}_{\tilde{X}})^\dagger_{i,i} [\alpha \mathbf{L}_{\tilde{Y}} - \mathbf{L}_{\tilde{X}}]_{i,j} = \frac{\alpha \mathbf{L}_{\tilde{Y}i,j} - \mathbf{L}_{\tilde{X}i,j}}{\text{Diag}(\mathbf{L}_{\tilde{X}})_{i,i}} \end{aligned}$$

Therefore,

$$\|\mathbf{z}_i\| = \sum_{j=1}^{n+1} \left(\left(\frac{\alpha \mathbf{L}_{Yi,j} - \mathbf{L}_{Xi,j}}{\text{Diag}(\mathbf{L}_X)_{i,i}} \right)^2 + \left(\frac{\alpha \mathbf{L}_{\tilde{Y}i,j} - \mathbf{L}_{\tilde{X}i,j}}{\text{Diag}(\mathbf{L}_{\tilde{X}})_{i,i}} \right)^2 - 2 \frac{(\alpha \mathbf{L}_{Yi,j} - \mathbf{L}_{Xi,j})(\alpha \mathbf{L}_{\tilde{Y}i,j} - \mathbf{L}_{\tilde{X}i,j})}{\text{Diag}(\mathbf{L}_X)_{i,i} \text{Diag}(\mathbf{L}_{\tilde{X}})_{i,i}} \right) \quad (25)$$

We bound the above summation by bounding each summand,

$$z_{ij} = \left(\frac{\alpha \mathbf{L}_{Yi,j} - \mathbf{L}_{Xi,j}}{\text{Diag}(\mathbf{L}_X)_{i,i}} \right)^2 + \left(\frac{\alpha \mathbf{L}_{\tilde{Y}i,j} - \mathbf{L}_{\tilde{X}i,j}}{\text{Diag}(\mathbf{L}_{\tilde{X}})_{i,i}} \right)^2 - 2 \frac{(\alpha \mathbf{L}_{Yi,j} - \mathbf{L}_{Xi,j})(\alpha \mathbf{L}_{\tilde{Y}i,j} - \mathbf{L}_{\tilde{X}i,j})}{\text{Diag}(\mathbf{L}_X)_{i,i} \text{Diag}(\mathbf{L}_{\tilde{X}})_{i,i}} \quad (26)$$

Recall that the $(n+1)$ th row of \mathbf{X} and \mathbf{Y} is $\mathbf{0}$. By equation (22),

$$\mathbf{L}_{X_{i,j}} = \begin{cases} \text{Diag}(\mathbf{L}_X)_{i,i} & \text{if } i = j \\ -\exp \left(-\frac{\|\mathbf{X}^T_i - \mathbf{X}^T_j\|^2}{2\sigma^2} \right) & \text{otherwise} \end{cases}$$

$$\mathbf{L}_{Y_{i,j}} = \begin{cases} \text{Diag}(\mathbf{L}_Y)_{i,i} & \text{if } i = j \\ -\exp \left(-\frac{\|\mathbf{Y}^T_i - \mathbf{Y}^T_j\|^2}{2\sigma^2} \right) & \text{otherwise} \end{cases}$$

where

$$\begin{aligned}\text{Diag}(\mathbf{L}_X)_{i,i} &= \sum_{k=1}^n \exp\left(-\frac{\|\mathbf{X}_i^T - \mathbf{X}_k^T\|^2}{2\sigma^2}\right) + \exp\left(-\frac{\|\mathbf{X}_i^T\|^2}{2\sigma^2}\right) - 1 \\ \text{Diag}(\mathbf{L}_Y)_{i,i} &= \sum_{k=1}^n \exp\left(-\frac{\|\mathbf{Y}_i^T - \mathbf{Y}_k^T\|^2}{2\sigma^2}\right) + \exp\left(-\frac{\|\mathbf{Y}_i^T\|^2}{2\sigma^2}\right) - 1\end{aligned}$$

Let \mathbf{v}_X and \mathbf{v}_Y be the additional records in the $(n+1)$ th rows of $\mathbf{L}_{\tilde{X}}$ and $\mathbf{L}_{\tilde{Y}}$ respectively. Then similarly,

$$\begin{aligned}\mathbf{L}_{\tilde{X},i,j} &= \begin{cases} \text{Diag}(\mathbf{L}_{\tilde{X}})_{i,i} & \text{if } i = j \\ -\exp\left(-\frac{\|\tilde{\mathbf{X}}_i^T - \tilde{\mathbf{X}}_j^T\|^2}{2\sigma^2}\right) & \text{if } i \neq j \end{cases} \\ \mathbf{L}_{\tilde{Y},i,j} &= \begin{cases} \text{Diag}(\mathbf{L}_{\tilde{Y}})_{i,i} & \text{if } i = j \\ -\exp\left(-\frac{\|\tilde{\mathbf{Y}}_i^T - \tilde{\mathbf{Y}}_j^T\|^2}{2\sigma^2}\right) & \text{if } i \neq j \end{cases}\end{aligned}$$

where

$$\begin{aligned}\text{Diag}(\mathbf{L}_{\tilde{X}})_{i,i} &= \sum_{k=1}^n \exp\left(-\frac{\|\mathbf{X}_i^T - \mathbf{X}_k^T\|^2}{2\sigma^2}\right) + \exp\left(-\frac{\|\tilde{\mathbf{X}}_i^T - \mathbf{v}_X\|^2}{2\sigma^2}\right) - 1 \\ \text{Diag}(\mathbf{L}_{\tilde{Y}})_{i,i} &= \sum_{k=1}^n \exp\left(-\frac{\|\mathbf{Y}_i^T - \mathbf{Y}_k^T\|^2}{2\sigma^2}\right) + \exp\left(-\frac{\|\tilde{\mathbf{Y}}_i^T - \mathbf{v}_Y\|^2}{2\sigma^2}\right) - 1\end{aligned}$$

We proceed to find upper and lower bounds for z_{ij} by cases.

Case 1: $i = j$. By equation (26), we have

$$\begin{aligned}z_{ii} &= \left(\frac{\alpha \mathbf{L}_{Y,i,i} - \mathbf{L}_{X,i,i}}{\text{Diag}(\mathbf{L}_X)_{i,i}}\right)^2 + \left(\frac{\alpha \mathbf{L}_{\tilde{Y},i,i} - \mathbf{L}_{\tilde{X},i,i}}{\text{Diag}(\mathbf{L}_{\tilde{X}})_{i,i}}\right)^2 - 2 \frac{(\alpha \mathbf{L}_{Y,i,i} - \mathbf{L}_{X,i,i})(\alpha \mathbf{L}_{\tilde{Y},i,i} - \mathbf{L}_{\tilde{X},i,i})}{\text{Diag}(\mathbf{L}_X)_{i,i} \text{Diag}(\mathbf{L}_{\tilde{X}})_{i,i}} \\ &= \frac{\alpha^2 \text{Diag}(\mathbf{L}_Y)_{i,i}^2 - 2\alpha \text{Diag}(\mathbf{L}_Y)_{i,i} \text{Diag}(\mathbf{L}_X)_{i,i} - \text{Diag}(\mathbf{L}_X)_{i,i}^2}{\text{Diag}(\mathbf{L}_X)_{i,i}^2} + \frac{\alpha^2 \text{Diag}(\mathbf{L}_{\tilde{Y}})_{i,i}^2 - 2\alpha \text{Diag}(\mathbf{L}_{\tilde{Y}})_{i,i} \text{Diag}(\mathbf{L}_{\tilde{X}})_{i,i} - \text{Diag}(\mathbf{L}_{\tilde{X}})_{i,i}^2}{\text{Diag}(\mathbf{L}_{\tilde{X}})_{i,i}^2} \\ &\quad - 2 \cdot \frac{\alpha^2 \text{Diag}(\mathbf{L}_Y)_{i,i} \text{Diag}(\mathbf{L}_{\tilde{Y}})_{i,i} - \alpha \text{Diag}(\mathbf{L}_Y)_{i,i} \text{Diag}(\mathbf{L}_{\tilde{X}})_{i,i} - \alpha \text{Diag}(\mathbf{L}_X)_{i,i} \text{Diag}(\mathbf{L}_{\tilde{Y}})_{i,i} + \text{Diag}(\mathbf{L}_X)_{i,i} \text{Diag}(\mathbf{L}_{\tilde{X}})_{i,i}}{\text{Diag}(\mathbf{L}_X)_{i,i} \text{Diag}(\mathbf{L}_{\tilde{X}})_{i,i}} \\ &= \alpha^2 \left(\frac{\text{Diag}(\mathbf{L}_Y)_{i,i}}{\text{Diag}(\mathbf{L}_X)_{i,i}}\right)^2 + \alpha^2 \left(\frac{\text{Diag}(\mathbf{L}_{\tilde{Y}})_{i,i}}{\text{Diag}(\mathbf{L}_{\tilde{X}})_{i,i}}\right)^2 - \frac{2\alpha^2 \text{Diag}(\mathbf{L}_Y)_{i,i} \text{Diag}(\mathbf{L}_{\tilde{Y}})_{i,i}}{\text{Diag}(\mathbf{L}_X)_{i,i} \text{Diag}(\mathbf{L}_{\tilde{X}})_{i,i}}\end{aligned}\quad (27)$$

By assumption, each row in \mathbf{X} , $\tilde{\mathbf{X}}$ is unit norm. Then by the law of cosines, we have

$$\begin{aligned}\|\mathbf{X}_i^T - \mathbf{X}_k^T\|^2 &= \|\mathbf{X}_i^T\|^2 + \|\mathbf{X}_k^T\|^2 - 2\|\mathbf{X}_i^T\|\|\mathbf{X}_k^T\|\cos\theta_{ik}^X = 2 - 2\cos\theta_{ik}^X \\ \|\tilde{\mathbf{X}}_i^T - \tilde{\mathbf{X}}_k^T\|^2 &= 2 - 2\cos\theta_{ik}^{\tilde{X}}\end{aligned}\quad (28)$$

Hence,

$$\begin{aligned}\sum_{k=1}^n \exp\left(-\frac{2-2(-1)}{2\sigma^2}\right) + \exp\left(-\frac{1}{2\sigma^2}\right) - 1 &\leq \text{Diag}(\mathbf{L}_X)_{i,i} \leq \sum_{k=1}^n \exp\left(-\frac{2-2(1)}{2\sigma^2}\right) + \exp\left(-\frac{1}{2\sigma^2}\right) - 1 \\ ne^{-\frac{2}{\sigma^2}} + e^{-\frac{1}{2\sigma^2}} - 1 &\leq \text{Diag}(\mathbf{L}_X)_{i,i} \leq n + e^{-\frac{1}{2\sigma^2}} - 1 \\ \sum_{k=1}^n \exp\left(-\frac{2-2(-1)}{2\sigma^2}\right) + \exp\left(-\frac{2-2(-1)}{2\sigma^2}\right) - 1 &\leq \text{Diag}(\mathbf{L}_{\tilde{X}})_{i,i} \leq \sum_{k=1}^n \exp\left(-\frac{2-2(1)}{2\sigma^2}\right) + \exp\left(-\frac{2-2(1)}{2\sigma^2}\right) - 1 \\ (n+1)e^{-\frac{2}{\sigma^2}} - 1 &\leq \text{Diag}(\mathbf{L}_{\tilde{X}})_{i,i} \leq n\end{aligned}\quad (29)$$

We now consider 2 possible cases for the structure of \mathbf{Y} , $\tilde{\mathbf{Y}}$:

Case A: Labels are one-hot encoded. Then similarly by the law of cosines, we have

$$\begin{aligned}\|\mathbf{Y}_i^T - \mathbf{Y}_k^T\|^2 &= 2 - 2\cos\theta_{ik}^{\mathbf{Y}} \\ \|\tilde{\mathbf{Y}}_i^T - \tilde{\mathbf{Y}}_k^T\|^2 &= 2 - 2\cos\theta_{ik}^{\tilde{\mathbf{Y}}}\end{aligned}\quad (30)$$

$$\begin{aligned}\sum_{k=1}^n \exp\left(-\frac{2-2(0)}{2\sigma^2}\right) + \exp\left(-\frac{1}{2\sigma^2}\right) - 1 &\leq \text{Diag}(\mathbf{L}_{\mathbf{Y}})_{i,i} \leq \sum_{k=1}^n \exp\left(-\frac{2-2(1)}{2\sigma^2}\right) + \exp\left(-\frac{1}{2\sigma^2}\right) - 1 \\ ne^{-\frac{1}{\sigma^2}} + e^{-\frac{1}{2\sigma^2}} - 1 &\leq \text{Diag}(\mathbf{L}_{\mathbf{Y}})_{i,i} \leq n + e^{-\frac{1}{2\sigma^2}} - 1 \\ \sum_{k=1}^n \exp\left(-\frac{2-2(0)}{2\sigma^2}\right) + \exp\left(-\frac{2-2(0)}{2\sigma^2}\right) - 1 &\leq \text{Diag}(\mathbf{L}_{\tilde{\mathbf{Y}}})_{i,i} \leq \sum_{k=1}^n \exp\left(-\frac{2-2(1)}{2\sigma^2}\right) + \exp\left(-\frac{2-2(1)}{2\sigma^2}\right) - 1 \\ (n+1)e^{-\frac{1}{\sigma^2}} - 1 &\leq \text{Diag}(\mathbf{L}_{\tilde{\mathbf{Y}}})_{i,i} \leq n\end{aligned}\quad (31)$$

Thus, an upper bound for z_{ii} is

$$\begin{aligned}z^{ii} &\leq \alpha^2 \left(\frac{n + e^{-\frac{1}{2\sigma^2}} - 1}{ne^{-\frac{2}{\sigma^2}} + e^{-\frac{1}{2\sigma^2}} - 1} \right)^2 + \alpha^2 \left(\frac{n}{(n+1)e^{-\frac{2}{\sigma^2}} - 1} \right)^2 - \frac{2\alpha^2 \left(ne^{-\frac{1}{\sigma^2}} + e^{-\frac{1}{2\sigma^2}} - 1 \right) \left((n+1)e^{-\frac{1}{\sigma^2}} - 1 \right)}{n \left(n + e^{-\frac{1}{2\sigma^2}} - 1 \right)} \\ &= z_{ii}^{\max}\end{aligned}\quad (32)$$

and a lower bound is

$$\begin{aligned}z_{ii} &\geq \alpha^2 \left(\frac{ne^{-\frac{1}{\sigma^2}} + e^{-\frac{1}{2\sigma^2}} - 1}{n + e^{-\frac{1}{2\sigma^2}} - 1} \right)^2 + \alpha^2 \left(\frac{(n+1)e^{-\frac{1}{\sigma^2}} - 1}{n} \right)^2 - \frac{2\alpha^2 n \left(n + e^{-\frac{1}{2\sigma^2}} - 1 \right)}{\left(ne^{-\frac{2}{\sigma^2}} + e^{-\frac{1}{2\sigma^2}} - 1 \right) \left((n+1)e^{-\frac{1}{\sigma^2}} - 1 \right)} \\ &= z_{ii}^{\min}\end{aligned}\quad (33)$$

Case B: $\mathbf{Y}, \tilde{\mathbf{Y}}$ are vectors of integer labels in $\{0, \dots, c\}$, where $c+1$ is the number of unique classes in the dataset. We then have the constraints $0 \leq \|\mathbf{Y}_i^T - \mathbf{Y}_k^T\|^2 \leq c^2$ which generate the following bounds,

$$\begin{aligned}\sum_{k=1}^n \exp\left(-\frac{c^2}{2\sigma^2}\right) + \exp\left(-\frac{c^2}{2\sigma^2}\right) - 1 &\leq \text{Diag}(\mathbf{L}_{\mathbf{Y}})_{i,i} \leq \sum_{k=1}^n \exp\left(-\frac{0}{2\sigma^2}\right) + \exp\left(-\frac{0}{2\sigma^2}\right) - 1 \\ (n+1)e^{-\frac{c^2}{2\sigma^2}} - 1 &\leq \text{Diag}(\mathbf{L}_{\mathbf{Y}})_{i,i} \leq n \\ \sum_{k=1}^n \exp\left(-\frac{c^2}{2\sigma^2}\right) + \exp\left(-\frac{c^2}{2\sigma^2}\right) - 1 &\leq \text{Diag}(\mathbf{L}_{\tilde{\mathbf{Y}}})_{i,i} \leq \sum_{k=1}^n \exp\left(-\frac{0}{2\sigma^2}\right) + \exp\left(-\frac{0}{2\sigma^2}\right) - 1 \\ (n+1)e^{-\frac{c^2}{2\sigma^2}} - 1 &\leq \text{Diag}(\mathbf{L}_{\tilde{\mathbf{Y}}})_{i,i} \leq n\end{aligned}\quad (34)$$

The corresponding bounds for z_{ii} are given by

$$\begin{aligned}z^{ii} &\leq \alpha^2 \left(\frac{n}{ne^{-\frac{2}{\sigma^2}} + e^{-\frac{1}{2\sigma^2}} - 1} \right)^2 + \alpha^2 \left(\frac{n}{(n+1)e^{-\frac{2}{\sigma^2}} - 1} \right)^2 - \frac{2\alpha^2 \left((n+1)e^{-\frac{c^2}{2\sigma^2}} - 1 \right)^2}{n \left(n + e^{-\frac{1}{2\sigma^2}} - 1 \right)} \\ &= z_{ii}^{\max}\end{aligned}\quad (35)$$

$$\begin{aligned}z_{ii} &\geq \alpha^2 \left(\frac{(n+1)e^{-\frac{c^2}{2\sigma^2}} - 1}{n + e^{-\frac{1}{2\sigma^2}} - 1} \right)^2 + \alpha^2 \left(\frac{(n+1)e^{-\frac{c^2}{2\sigma^2}} - 1}{n} \right)^2 - \frac{2\alpha^2 n^2}{\left(ne^{-\frac{2}{\sigma^2}} + e^{-\frac{1}{2\sigma^2}} - 1 \right) \left((n+1)e^{-\frac{1}{\sigma^2}} - 1 \right)} \\ &= z_{ii}^{\min}\end{aligned}\quad (36)$$

Case 2: $i \neq j$. By equation (26), we have

$$\begin{aligned}
z_{ij} &= \left(\frac{-\alpha \exp\left(-\frac{\|\mathbf{Y}_i^T - \mathbf{Y}_j^T\|^2}{2\sigma^2}\right) + \exp\left(-\frac{\|\mathbf{X}_i^T - \mathbf{X}_j^T\|^2}{2\sigma^2}\right)}{\text{Diag}(\mathbf{L}_X)_{i,i}} \right)^2 + \left(\frac{-\alpha \exp\left(-\frac{\|\tilde{\mathbf{Y}}_i^T - \tilde{\mathbf{Y}}_j^T\|^2}{2\sigma^2}\right) + \exp\left(-\frac{\|\tilde{\mathbf{X}}_i^T - \tilde{\mathbf{X}}_j^T\|^2}{2\sigma^2}\right)}{\text{Diag}(\mathbf{L}_{\tilde{X}})_{i,i}} \right)^2 \\
&\quad - 2 \cdot \frac{\left(-\alpha \exp\left(-\frac{\|\mathbf{Y}_i^T - \mathbf{Y}_j^T\|^2}{2\sigma^2}\right) + \exp\left(-\frac{\|\mathbf{X}_i^T - \mathbf{X}_j^T\|^2}{2\sigma^2}\right)\right) \left(-\alpha \exp\left(-\frac{\|\tilde{\mathbf{Y}}_i^T - \tilde{\mathbf{Y}}_j^T\|^2}{2\sigma^2}\right) + \exp\left(-\frac{\|\tilde{\mathbf{X}}_i^T - \tilde{\mathbf{X}}_j^T\|^2}{2\sigma^2}\right)\right)}{\text{Diag}(\mathbf{L}_X)_{i,i} \text{Diag}(\mathbf{L}_{\tilde{X}})_{i,i}} \\
&= \frac{\alpha^2 \exp\left(-\frac{\|\mathbf{Y}_i^T - \mathbf{Y}_j^T\|^2}{\sigma^2}\right) + \exp\left(-\frac{\|\mathbf{X}_i^T - \mathbf{X}_j^T\|^2}{\sigma^2}\right)}{\text{Diag}(\mathbf{L}_X)_{i,i}} - \frac{2\alpha \exp\left(-\frac{\|\mathbf{Y}_i^T - \mathbf{Y}_j^T\|^2 + \|\mathbf{X}_i^T - \mathbf{X}_j^T\|^2}{2\sigma^2}\right)}{\text{Diag}(\mathbf{L}_X)_{i,i}} \\
&\quad + \frac{\alpha^2 \exp\left(-\frac{\|\tilde{\mathbf{Y}}_i^T - \tilde{\mathbf{Y}}_j^T\|^2}{\sigma^2}\right) + \exp\left(-\frac{\|\tilde{\mathbf{X}}_i^T - \tilde{\mathbf{X}}_j^T\|^2}{\sigma^2}\right)}{\text{Diag}(\mathbf{L}_{\tilde{X}})_{i,i}} - \frac{2\alpha \exp\left(-\frac{\|\tilde{\mathbf{Y}}_i^T - \tilde{\mathbf{Y}}_j^T\|^2 + \|\tilde{\mathbf{X}}_i^T - \tilde{\mathbf{X}}_j^T\|^2}{2\sigma^2}\right)}{\text{Diag}(\mathbf{L}_{\tilde{X}})_{i,i}} \\
&\quad - 2 \cdot \frac{\alpha^2 \exp\left(-\frac{\|\mathbf{Y}_i^T - \mathbf{Y}_j^T\|^2 + \|\tilde{\mathbf{Y}}_i^T + \tilde{\mathbf{Y}}_j^T\|^2}{2\sigma^2}\right) + \exp\left(-\frac{\|\mathbf{X}_i^T - \mathbf{X}_j^T\|^2 + \|\tilde{\mathbf{X}}_i^T - \tilde{\mathbf{X}}_j^T\|^2}{2\sigma^2}\right)}{\text{Diag}(\mathbf{L}_X)_{i,i} \text{Diag}(\mathbf{L}_{\tilde{X}})_{i,i}} \\
&\quad + 2\alpha \cdot \frac{\exp\left(-\frac{\|\mathbf{Y}_i^T - \mathbf{Y}_j^T\|^2 + \|\tilde{\mathbf{X}}_i^T - \tilde{\mathbf{X}}_j^T\|^2}{2\sigma^2}\right) + \exp\left(-\frac{\|\tilde{\mathbf{Y}}_i^T - \tilde{\mathbf{Y}}_j^T\|^2 + \|\mathbf{X}_i^T - \mathbf{X}_j^T\|^2}{2\sigma^2}\right)}{\text{Diag}(\mathbf{L}_X)_{i,i} \text{Diag}(\mathbf{L}_{\tilde{X}})_{i,i}}
\end{aligned}$$

We repeat the case-wise analysis for possible $\mathbf{Y}, \tilde{\mathbf{Y}}$.

Case A: By the constraints in equations (29) and (31), we have

$$\begin{aligned}
z_{ij} &\leq \frac{\alpha^2 \exp\left(-\frac{2-2(1)}{\sigma^2}\right) + \exp\left(-\frac{2-2(1)}{\sigma^2}\right)}{ne^{-\frac{2}{\sigma^2}} + e^{-\frac{1}{2\sigma^2}} - 1} - \frac{2\alpha \exp\left(-\frac{2-2(0)+2-2(-1)}{2\sigma^2}\right)}{n + e^{-\frac{1}{2\sigma^2}} - 1} \\
&\quad + \frac{\alpha^2 \exp\left(-\frac{2-2(1)}{\sigma^2}\right) + \exp\left(-\frac{2-2(1)}{\sigma^2}\right)}{(n+1)e^{-\frac{2}{\sigma^2}} - 1} - \frac{2\alpha \exp\left(-\frac{2-2(0)+2-2(-1)}{2\sigma^2}\right)}{n} \\
&\quad - 2 \cdot \frac{\alpha^2 \exp\left(-\frac{2-2(0)+2-2(0)}{2\sigma^2}\right) + \exp\left(-\frac{2-2(-1)+2-2(-1)}{2\sigma^2}\right)}{n(n + e^{-\frac{1}{2\sigma^2}} - 1)} + \frac{2\alpha \left[\exp\left(-\frac{2-2(1)+2-2(1)}{2\sigma^2}\right) + \exp\left(-\frac{2-2(1)+2-2(1)}{2\sigma^2}\right) \right]}{\left(ne^{-\frac{2}{\sigma^2}} + e^{-\frac{1}{2\sigma^2}} - 1\right) \left((n+1)e^{-\frac{2}{\sigma^2}} - 1\right)} \\
&= \frac{\alpha^2 + 1}{ne^{-\frac{2}{\sigma^2}} + e^{-\frac{1}{2\sigma^2}} - 1} - \frac{2\alpha e^{-\frac{3}{2\sigma^2}}}{n + e^{-\frac{1}{2\sigma^2}} - 1} + \frac{\alpha^2 + 1}{(n+1)e^{-\frac{2}{\sigma^2}} - 1} - \frac{2\alpha e^{-\frac{3}{2\sigma^2}}}{n} \\
&\quad - \frac{2\left(\alpha^2 e^{-\frac{2}{\sigma^2}} + e^{-\frac{4}{\sigma^2}}\right)}{n(n + e^{-\frac{1}{2\sigma^2}} - 1)} + \frac{4\alpha}{\left(ne^{-\frac{2}{\sigma^2}} + e^{-\frac{1}{2\sigma^2}} - 1\right) \left((n+1)e^{-\frac{2}{\sigma^2}} - 1\right)} \\
&= z_{ij}^{\max}
\end{aligned} \tag{37}$$

$$\begin{aligned}
z_{ij} &\geq \frac{\alpha^2 \exp\left(-\frac{2-2(0)}{\sigma^2}\right) + \exp\left(-\frac{2-2(-1)}{\sigma^2}\right)}{n + e^{-\frac{1}{2\sigma^2}} - 1} - \frac{2\alpha \exp\left(-\frac{2-2(1)+2-2(1)}{2\sigma^2}\right)}{ne^{-\frac{2}{\sigma^2}} + e^{-\frac{1}{2\sigma^2}} - 1} \\
&+ \frac{\alpha^2 \exp\left(-\frac{2-2(0)}{\sigma^2}\right) + \exp\left(-\frac{2-2(-1)}{\sigma^2}\right)}{n} - \frac{2\alpha \exp\left(-\frac{2-2(1)+2-2(1)}{2\sigma^2}\right)}{(n+1)e^{-\frac{2}{\sigma^2}} - 1} \\
&- 2 \cdot \frac{\alpha^2 \exp\left(-\frac{2-2(1)+2-2(1)}{2\sigma^2}\right) + \exp\left(-\frac{2-2(1)+2-2(1)}{2\sigma^2}\right)}{\left(ne^{-\frac{2}{\sigma^2}} + e^{-\frac{1}{2\sigma^2}} - 1\right)\left((n+1)e^{-\frac{2}{\sigma^2}} - 1\right)} + 2\alpha \cdot \frac{\exp\left(-\frac{2-2(0)+2-2(-1)}{2\sigma^2}\right) + \exp\left(-\frac{2-2(0)+2-2(-1)}{2\sigma^2}\right)}{n\left(n + e^{-\frac{1}{2\sigma^2}} - 1\right)} \\
&= \frac{\alpha^2 e^{-\frac{2}{\sigma^2}} + e^{-\frac{4}{\sigma^2}}}{n + e^{-\frac{1}{2\sigma^2}} - 1} - \frac{2\alpha}{ne^{-\frac{2}{\sigma^2}} + e^{-\frac{1}{2\sigma^2}} - 1} + \frac{\alpha^2 e^{-\frac{2}{\sigma^2}} + e^{-\frac{4}{\sigma^2}}}{n} - \frac{2\alpha}{(n+1)e^{-\frac{2}{\sigma^2}} - 1} \\
&- \frac{2(\alpha^2 + 1)}{\left(ne^{-\frac{2}{\sigma^2}} + e^{-\frac{1}{2\sigma^2}} - 1\right)\left((n+1)e^{-\frac{2}{\sigma^2}} - 1\right)} + \frac{4\alpha e^{-\frac{3}{\sigma^2}}}{n\left(n + e^{-\frac{1}{2\sigma^2}} - 1\right)} \\
&= z_{ij}^{\min}
\end{aligned} \tag{38}$$

Case B: By the constraints in equations (29) and (34), we have

$$\begin{aligned}
z_{ij} &\leq \frac{\alpha^2 + 1}{ne^{-\frac{2}{\sigma^2}} + e^{-\frac{1}{2\sigma^2}} - 1} - \frac{2\alpha \exp\left(-\frac{c^2+4}{2\sigma^2}\right)}{n + e^{-\frac{1}{2\sigma^2}} - 1} + \frac{\alpha^2 + 1}{(n+1)e^{-\frac{2}{\sigma^2}} - 1} - \frac{2\alpha \exp\left(-\frac{c^2+4}{2\sigma^2}\right)}{n} \\
&- \frac{2\left(\alpha^2 e^{-\frac{c^2}{\sigma^2}} + e^{-\frac{4}{\sigma^2}}\right)}{n\left(n + e^{-\frac{1}{2\sigma^2}} - 1\right)} + \frac{4\alpha}{\left(ne^{-\frac{2}{\sigma^2}} + e^{-\frac{1}{2\sigma^2}} - 1\right)\left((n+1)e^{-\frac{2}{\sigma^2}} - 1\right)} \\
&= z_{ij}^{\max}
\end{aligned} \tag{39}$$

$$\begin{aligned}
z_{ij} &\geq \frac{\alpha^2 e^{-\frac{c^2}{\sigma^2}} + e^{-\frac{4}{\sigma^2}}}{n + e^{-\frac{1}{2\sigma^2}} - 1} - \frac{2\alpha}{ne^{-\frac{2}{\sigma^2}} + e^{-\frac{1}{2\sigma^2}} - 1} + \frac{\alpha^2 e^{-\frac{c^2}{\sigma^2}} + e^{-\frac{4}{\sigma^2}}}{n} - \frac{2\alpha}{(n+1)e^{-\frac{2}{\sigma^2}} - 1} \\
&- \frac{2(\alpha^2 + 1)}{\left(ne^{-\frac{2}{\sigma^2}} + e^{-\frac{1}{2\sigma^2}} - 1\right)\left((n+1)e^{-\frac{2}{\sigma^2}} - 1\right)} + \frac{4\alpha e^{-\frac{c^2+4}{\sigma^2}}}{n\left(n + e^{-\frac{1}{2\sigma^2}} - 1\right)} \\
&= z_{ij}^{\min}
\end{aligned} \tag{40}$$

Then by equation (25), an upper bound for $\|\mathbf{z}_i\|$ is given by

$$\begin{aligned}
\|\mathbf{z}_i\| &\leq \sum_{j \neq i} z_{ij}^{\max} + z_{ii}^{\max} \\
&= nz_{ij}^{\max} + z_{ii}^{\max} \\
&= \phi^{\max}
\end{aligned} \tag{41}$$

and a lower bound is given by

$$\begin{aligned}
\|\mathbf{z}_i\| &\geq \sum_{j \neq i} z_{ij}^{\min} + z_{ii}^{\min} \\
&= nz_{ij}^{\min} + z_{ii}^{\min} \\
&= \phi^{\min}
\end{aligned} \tag{42}$$

Using these constants, we obtain an upper bound on $LS_f(\mathbf{X})$ as shown in equation (24).

B CONVERGENCE RATE

$$M'(\mathbf{X}^*) = - \left[\frac{\partial^2 g_{\text{concave}}(\Omega)}{\partial \Omega \partial \Omega^T} \Big|_{\Omega = \mathbf{X}^*} \right] \left[\frac{\partial^2 f_{\text{convex}}(\mathbf{X})}{\partial \mathbf{X} \partial \mathbf{X}^T} \Big|_{\mathbf{X} = \mathbf{X}^*} \right]^{-1} \quad (43)$$

If the concave Hessian has small curvature compared to the convex Hessian in the neighborhood of an optima, then CCCP will generally have a superlinear convergence like quasi-Newton methods. For a fixed z_0 , the model is a function of two variables and therefore the local curvature of the concave Hessian is given by

$$\frac{|H(g_{\text{concave}}(\Omega))|_{\Omega = \mathbf{X}^*}|}{(1 + [g_{(x_0)}]^2 + [g_{(y_0)}]^2)^2}$$

Note that in numerator, $||$ refers to the determinant. Therefore if this term is much smaller compared to the corresponding local curvature of the convex function given by

$$\frac{|H(f_{\text{convex}}(\mathbf{X}))|_{\mathbf{X} = \mathbf{X}^*}|}{(1 + [f_{(x_0)}]^2 + [f_{(y_0)}]^2)^2}$$

then we have super-linear convergence. Note that $f_{(x_0)}, f_{(y_0)}, g_{(x_0)}$ and $g_{(y_0)}$ are the partial derivatives of f_{convex} and g_{concave} respectively.

C MULTIDIMENSIONAL LAPLACE MECHANISM

For a multidimensional real-valued query function $q : \mathcal{D} \mapsto \mathbb{R}^d$ with sensitivity Δ , the Laplace mechanism will output

$$K(D) := q(D) + \text{Lap} \left(\frac{\Delta}{\epsilon} \right)^d \quad (44)$$

$$= \left(q_1(D) + \text{Lap} \left(\frac{\Delta}{\epsilon} \right)^d, \dots, q_d(D) + \text{Lap} \left(\frac{\Delta}{\epsilon} \right)^d \right) \quad (45)$$

where $\text{Lap}(\lambda)$ is a random variable with probability density function $f(x) = \frac{1}{2\lambda} e^{-\frac{|x|}{\lambda}}, \forall x \in \mathbb{R}$, and all d Laplace random variables are independent.

D BIG PICTURE OF OUR PROOF STRATEGY

This is a condensed big picture of the strategy used for the proofs provided in previous appendices. By the union bound, we have

$$\begin{aligned} \mathbb{P}(LS_f(\mathbf{X}) > \sqrt{t}) &= \mathbb{P} \left(\max_{\tilde{\mathbf{X}}:d(\mathbf{X}, \tilde{\mathbf{X}})=1} \|f(\mathbf{X}) - f(\tilde{\mathbf{X}})\|_F > \sqrt{t} \right) \\ &= \mathbb{P} \left(\bigcup_{\tilde{\mathbf{X}}:d(\mathbf{X}, \tilde{\mathbf{X}})=1} \{ \|f(\mathbf{X}) - f(\tilde{\mathbf{X}})\|_F > \sqrt{t} \} \right) \\ &\leq \sum_{\tilde{\mathbf{X}}:d(\mathbf{X}, \tilde{\mathbf{X}})=1} \mathbb{P}(\|f(\mathbf{X}) - f(\tilde{\mathbf{X}})\|_F > \sqrt{t}) \\ &\leq \sum_{\tilde{\mathbf{X}}:d(\mathbf{X}, \tilde{\mathbf{X}})=1} \beta \end{aligned} \quad (46)$$

Then for very small β , we can conclude with high probability $1 - \sum_{\tilde{\mathbf{X}}:d(\mathbf{X}, \tilde{\mathbf{X}})=1} \beta$ that $\|f(\mathbf{X}) - f(\tilde{\mathbf{X}})\| \leq \sqrt{t}$.

The tightest such bound is thus given by minimizing \sqrt{t} subject to the constraints

$$\exp \left(\frac{k \left(\sum_{i=1}^n \|\mathbf{z}_i\|^2 \right)^2}{2 \sum_{i=1}^n \|\mathbf{z}_i\|^4} \sqrt{1 + \frac{8t}{k \sigma_q^2 \sum_{i=1}^n \|\mathbf{z}_i\|^2}} \right) = \beta \quad (47)$$

$$t \geq 0 \quad (48)$$

where constraint (47) is derived from properties of the approximate distribution of $P(LS_f(\mathbf{X}) > \sqrt{t})$ and constraint (48) must hold since $\|f(\mathbf{X}) - f(\tilde{\mathbf{X}})\|_F$ is always nonnegative. The resulting optimal bound in Theorem 1 is nonnegative when

$$0 < \beta \leq \exp \left(- \frac{4k \left(\sum_{i=1}^n \|\mathbf{z}_i\|^2 \right)^2}{\sum_{i=1}^n \|\mathbf{z}_i\|^4} \right)$$

The derivation of a constant bound in Corollary 1.1 relies on expanding the definition of the laplacian matrices in (5.1) and applying law of cosines for the difference of vectors.

E SUMMARY OF OUR DATA-INDEPENDENT CONSTANTS REQUIRED FOR COMPUTING UPPER BOUND ON GLOBAL SENSITIVITY

Computation of data independent upper and lower bounds on $\|\mathbf{z}_i\|$ such that $\phi^{\min} \leq \|\mathbf{z}_i\| \leq \phi^{\max}$ in either of the following 2 cases:

Case 1: Class labels are one-hot encoded.

1.
$$z_{ij}^{\min} = \frac{\alpha^2 e^{-\frac{2}{\sigma^2}} + e^{-\frac{4}{\sigma^2}}}{n + e^{-\frac{1}{2\sigma^2}} - 1} - \frac{2\alpha}{ne^{-\frac{2}{\sigma^2}} + e^{-\frac{1}{2\sigma^2}} - 1} + \frac{\alpha^2 e^{-\frac{2}{\sigma^2}} + e^{-\frac{4}{\sigma^2}}}{n} - \frac{2\alpha}{(n+1)e^{-\frac{2}{\sigma^2}} - 1}$$

$$- \frac{2(\alpha^2 + 1)}{\left(ne^{-\frac{2}{\sigma^2}} + e^{-\frac{1}{2\sigma^2}} - 1 \right) \left((n+1)e^{-\frac{2}{\sigma^2}} - 1 \right)} + \frac{4\alpha e^{-\frac{3}{\sigma^2}}}{n \left(ne^{-\frac{2}{\sigma^2}} + e^{-\frac{1}{2\sigma^2}} - 1 \right)}$$
2.
$$z_{ij}^{\max} = \frac{\alpha^2 + 1}{ne^{-\frac{2}{\sigma^2}} + e^{-\frac{1}{2\sigma^2}} - 1} - \frac{2\alpha e^{-\frac{3}{\sigma^2}}}{n + e^{-\frac{1}{2\sigma^2}} - 1} + \frac{\alpha^2 + 1}{(n+1)e^{-\frac{2}{\sigma^2}} - 1} - \frac{2\alpha e^{-\frac{3}{\sigma^2}}}{n}$$

$$- \frac{2 \left(\alpha^2 e^{-\frac{2}{\sigma^2}} + e^{-\frac{4}{\sigma^2}} \right)}{n \left(ne^{-\frac{1}{2\sigma^2}} - 1 \right)} + \frac{4\alpha}{\left(ne^{-\frac{2}{\sigma^2}} + e^{-\frac{1}{2\sigma^2}} - 1 \right) \left((n+1)e^{-\frac{2}{\sigma^2}} - 1 \right)}$$
3.
$$z_{ii}^{\min} = \alpha^2 \left(\frac{ne^{-\frac{1}{\sigma^2}} + e^{-\frac{1}{2\sigma^2}} - 1}{n + e^{-\frac{1}{2\sigma^2}} - 1} \right)^2 + \alpha^2 \left(\frac{(n+1)e^{-\frac{1}{\sigma^2}} - 1}{n} \right)^2 - \frac{2\alpha^2 n \left(ne^{-\frac{1}{2\sigma^2}} - 1 \right)}{\left(ne^{-\frac{2}{\sigma^2}} + e^{-\frac{1}{2\sigma^2}} - 1 \right) \left((n+1)e^{-\frac{1}{\sigma^2}} - 1 \right)}$$
4.
$$z_{ii}^{\max} = \alpha^2 \left(\frac{n + e^{-\frac{1}{2\sigma^2}} - 1}{ne^{-\frac{2}{\sigma^2}} + e^{-\frac{1}{2\sigma^2}} - 1} \right)^2 + \alpha^2 \left(\frac{n}{(n+1)e^{-\frac{2}{\sigma^2}} - 1} \right)^2 - \frac{2\alpha^2 \left(ne^{-\frac{1}{\sigma^2}} + e^{-\frac{1}{2\sigma^2}} - 1 \right) \left((n+1)e^{-\frac{1}{\sigma^2}} - 1 \right)}{n \left(ne^{-\frac{1}{2\sigma^2}} - 1 \right)}$$
5. $\phi^{\max} = n z_{ij}^{\max} + z_{ii}^{\max}$
6. $\phi^{\min} = n z_{ij}^{\min} + z_{ii}^{\min}$

Case 2: Class labels are integers from $\{0, \dots, c\}$, where $c + 1$ is the number of classes in the dataset. as

1.
$$z_{ij}^{\min} = \alpha^2 \left(\frac{(n+1)e^{-\frac{c^2}{2\sigma^2}} - 1}{n + e^{-\frac{1}{2\sigma^2}} - 1} \right)^2 + \alpha^2 \left(\frac{(n+1)e^{-\frac{c^2}{2\sigma^2}} - 1}{n} \right)^2 - \frac{2\alpha^2 n^2}{\left(ne^{-\frac{2}{\sigma^2}} + e^{-\frac{1}{2\sigma^2}} - 1 \right) \left((n+1)e^{-\frac{1}{\sigma^2}} - 1 \right)}$$

$$2. z_{ij}^{\max} = \alpha^2 \left(\frac{n}{ne^{-\frac{2}{\sigma^2}} + e^{-\frac{1}{2\sigma^2}} - 1} \right)^2 + \alpha^2 \left(\frac{n}{(n+1)e^{-\frac{2}{\sigma^2}} - 1} \right)^2 - \frac{2\alpha^2 \left((n+1)e^{-\frac{1}{2\sigma^2}} - 1 \right)^2}{n \left(n + e^{-\frac{1}{2\sigma^2}} - 1 \right)}$$

$$3. z_{ii}^{\min} = \alpha^2 \left(\frac{ne^{-\frac{1}{\sigma^2}} + e^{-\frac{1}{2\sigma^2}} - 1}{n + e^{-\frac{1}{2\sigma^2}} - 1} \right)^2 + \alpha^2 \left(\frac{(n+1)e^{-\frac{1}{\sigma^2}} - 1}{n} \right)^2 - \frac{2\alpha^2 n \left(n + e^{-\frac{1}{2\sigma^2}} - 1 \right)}{\left(ne^{-\frac{2}{\sigma^2}} + e^{-\frac{1}{2\sigma^2}} - 1 \right) \left((n+1)e^{-\frac{1}{\sigma^2}} - 1 \right)}$$

$$4. z_{ii}^{\max} = \alpha^2 \left(\frac{n + e^{-\frac{1}{2\sigma^2}} - 1}{ne^{-\frac{2}{\sigma^2}} + e^{-\frac{1}{2\sigma^2}} - 1} \right)^2 + \alpha^2 \left(\frac{n}{(n+1)e^{-\frac{2}{\sigma^2}} - 1} \right)^2 - \frac{2\alpha^2 \left(ne^{-\frac{1}{\sigma^2}} + e^{-\frac{1}{2\sigma^2}} - 1 \right) \left((n+1)e^{-\frac{1}{\sigma^2}} - 1 \right)}{n \left(n + e^{-\frac{1}{2\sigma^2}} - 1 \right)}$$

$$5. \phi^{\max} = nz_{ij}^{\max} + z_{ii}^{\max}$$

$$6. \phi^{\min} = nz_{ij}^{\min} + z_{ii}^{\min}$$